

Search for diboson resonances with boson-tagged jets in pp collisions at $\sqrt{s}=13$ TeV with the ATLAS detector

Article (Published Version)

Allbrooke, B M M, Asquith, L, Cerri, A, Chavez Barajas, C A, De Santo, A, Salvatore, F, Santoyo Castillo, I, Suruliz, K, Sutton, M R, Vivarelli, I and The ATLAS Collaboration, (2017) Search for diboson resonances with boson-tagged jets in pp collisions at $\sqrt{s}=13$ TeV with the ATLAS detector. Physics Letters B, 777. pp. 91-113. ISSN 0370-2693

This version is available from Sussex Research Online: <http://sro.sussex.ac.uk/id/eprint/73562/>

This document is made available in accordance with publisher policies and may differ from the published version or from the version of record. If you wish to cite this item you are advised to consult the publisher's version. Please see the URL above for details on accessing the published version.

Copyright and reuse:

Sussex Research Online is a digital repository of the research output of the University.

Copyright and all moral rights to the version of the paper presented here belong to the individual author(s) and/or other copyright owners. To the extent reasonable and practicable, the material made available in SRO has been checked for eligibility before being made available.

Copies of full text items generally can be reproduced, displayed or performed and given to third parties in any format or medium for personal research or study, educational, or not-for-profit purposes without prior permission or charge, provided that the authors, title and full bibliographic details are credited, a hyperlink and/or URL is given for the original metadata page and the content is not changed in any way.



Search for diboson resonances with boson-tagged jets in pp collisions at $\sqrt{s} = 13$ TeV with the ATLAS detector

The ATLAS Collaboration ^{*}

ARTICLE INFO

Article history:

Received 16 August 2017
Received in revised form 4 December 2017
Accepted 5 December 2017
Available online 7 December 2017
Editor: M. Doser

ABSTRACT

Narrow resonances decaying into WW , WZ or ZZ boson pairs are searched for in 36.7 fb^{-1} of proton–proton collision data at a centre-of-mass energy of $\sqrt{s} = 13$ TeV recorded with the ATLAS detector at the Large Hadron Collider in 2015 and 2016. The diboson system is reconstructed using pairs of large-radius jets with high transverse momentum and tagged as compatible with the hadronic decay of high-momentum W or Z bosons, using jet mass and substructure properties. The search is sensitive to diboson resonances with masses in the range 1.2–5.0 TeV. No significant excess is observed in any signal region. Exclusion limits are set at the 95% confidence level on the production cross section times branching ratio to dibosons for a range of theories beyond the Standard Model. Model-dependent lower limits on the mass of new gauge bosons are set, with the highest limit set at 3.5 TeV in the context of mass-degenerate resonances that couple predominantly to bosons.

© 2017 The Author(s). Published by Elsevier B.V. This is an open access article under the CC BY license (<http://creativecommons.org/licenses/by/4.0/>). Funded by SCOAP³.

1. Introduction

A major goal of the physics programme at the Large Hadron Collider (LHC) is the search for new phenomena that may become visible in high-energy proton–proton (pp) collisions. One possible signature of such new phenomena is the production of a heavy resonance with the subsequent decay into a final state consisting of a pair of vector bosons (WW , WZ , ZZ). Many models of physics beyond the Standard Model (SM) predict such a signature. These include extensions to the SM scalar sector as in the two-Higgs-doublet model (2HDM) [1] that predict new spin-0 resonances, composite-Higgs models [2–4] and models motivated by Grand Unified Theories [5–7] that predict new W' spin-1 resonances, and warped extra dimensions Randall–Sundrum (RS) models [8–10] that predict spin-2 Kaluza–Klein (KK) excitations of the graviton, G_{KK} . The heavy vector triplet (HVT) [11,12] phenomenological Lagrangian approach provides a more model-independent framework for interpretation of spin-1 diboson resonances.

The search presented here focuses on TeV-scale resonances that decay into pairs of high-momentum vector bosons which, in turn, decay hadronically. The decay products of each of those vector bosons are collimated due to the high Lorentz boost and are typically contained in a single jet with radius $R = 1.0$. While the use of hadronic decays of the vector bosons benefits from the largest branching ratio (67% for W and 70% for Z bosons) amongst the possible final states, it suffers from a large background contami-

nation from the production of multijet events. However, this contamination can be mitigated with jet substructure techniques that exploit the two-body nature of $V \rightarrow qq$ decays (with $V = W$ or Z).

Previous searches for diboson resonances were carried out by the ATLAS and CMS collaborations with pp collisions at $\sqrt{s} = 7$, 8 and 13 TeV. These include fully leptonic ($\ell\ell\ell\ell$, $\ell\nu\ell\ell$) [13–16], semileptonic ($\nu\nu qq$, $\ell\nu qq$, $\ell\ell qq$) [17–19] and fully hadronic ($qqqq$) VV [17,19] final states. By combining the results of searches in the $\nu\nu qq$, $\ell\nu qq$, $\ell\ell qq$ and $qqqq$ channels, the ATLAS Collaboration [17] set a lower bound of 2.60 TeV on the mass of a spin-1 resonance at the 95% confidence level, in the context of the HVT model B with $g_V = 3$ (described in Section 2). When interpreted in the context of the bulk RS model with a spin-2 KK graviton and $k/\bar{M}_{\text{Pl}} = 1$, this lower mass bound is 1.10 TeV. The results presented here benefit from an integrated luminosity of 36.7 fb^{-1} , which is an order of magnitude larger than was available for the previous search in the fully hadronic final state at $\sqrt{s} = 13$ TeV [17].

2. Signal models

The analysis results are interpreted in terms of different models that predict the production of heavy resonances with either spin 0, spin 1 or spin 2. In the case of the spin-0 interpretation, a heavy scalar is produced via gluon–gluon fusion with subsequent decay into a pair of vector bosons. For this empirical model, the width of the signal in the diboson mass distribution is assumed to be dominated by the experimental resolution. The width of a Gaussian distribution characterising the mass resolution after full event selection ranges from approximately 3% to 2% as the resonance mass

^{*} E-mail address: atlas.publications@cern.ch.

increases from 1.2 to 5.0 TeV. The spin-0 model is referred to as the heavy scalar model in the rest of this Letter.

In the HVT phenomenological Lagrangian model, a new heavy vector triplet (W' , Z') is introduced, with the new gauge bosons degenerate in mass (also denoted by V' in the following). The couplings between those bosons and SM particles are described in a general manner, thereby allowing a broad class of models to be encompassed by this approach. The new triplet field interacts with the Higgs field and thus with the longitudinally polarised W and Z bosons by virtue of the equivalence theorem [20–22]. The strength of the coupling to the Higgs field, and thus SM gauge bosons, is controlled by the parameter combination $g_V c_H$, where c_H is a multiplicative constant used to parameterise potential deviations from the typical strength of triplet interactions to SM vector bosons, taken to be g_V . Coupling of the triplet field to SM fermions is set by the expression $g^2 c_F / g_V$, where g is the SM $SU(2)_L$ gauge coupling and, like for the coupling to the Higgs field, c_F is a multiplicative factor that modifies the typical coupling of the triplet field to fermions. The HVT model A with $g_V = 1$, $c_H \simeq -g^2/g_V^2$ and $c_F \simeq 1$ [11] is used as a benchmark. In this model, the new triplet field couples weakly to SM particles and arises from an extension of the SM gauge group. Branching ratios for $W' \rightarrow WZ$ and $Z' \rightarrow WW$ are approximately 2.0% each. The intrinsic width Γ of the new bosons is approximately 2.5% of the mass, which results in observable mass peaks with a width dominated by the experimental resolution. In this model, the dominant decay modes are into fermion pairs and searches in the $\ell\ell$ and $\ell\nu$ final states [23, 24] provide the best sensitivity. The calculated production cross section times branching ratio ($\sigma \times \mathcal{B}$) values for $W' \rightarrow WZ$ with W and Z bosons decaying hadronically are 8.3 and 0.75 fb for W' masses of 2 and 3 TeV, respectively. Corresponding values for $Z' \rightarrow WW$ are 3.8 and 0.34 fb.

The HVT model B with $g_V = 3$ and $c_H \simeq c_F \simeq 1$ [11] is used as another benchmark. This model describes scenarios in which strong dynamics give rise to the SM Higgs boson and naturally include a new heavy vector triplet field with electroweak quantum numbers. The constants c_H and c_F are approximately unity, and couplings to fermions are suppressed, giving rise to larger branching ratios ($\sim 50\%$) for either $W' \rightarrow WZ$ or $Z' \rightarrow WW$ decays than in model A. Resonance widths and experimental signatures are similar to those obtained for model A and the predicted $\sigma \times \mathcal{B}$ values for $W' \rightarrow WZ$ with hadronic W and Z decays are 13 and 1.3 fb for W' masses of 2 and 3 TeV, respectively. Corresponding values for $Z' \rightarrow WW$ are 6.0 and 0.55 fb.

The RS model with one warped extra dimension predicts the existence of spin-2 Kaluza–Klein excitations of the graviton, with the lowest mode being considered in this search. While the original RS model [8] (often referred to as RS1) is constructed with all SM fields confined to a four-dimensional brane (the “TeV brane”), the bulk RS model [8,9] employed here allows those fields to propagate in the extra-dimensional bulk between the TeV brane and the Planck brane. Although ruled out by precision electroweak and flavour measurements, the RS1 model is used as a benchmark model to interpret diphoton and dilepton resonance searches due to the sizeable G_{KK} couplings to light fermions in that model. In the bulk RS model, those couplings are suppressed and decays into final states involving heavy fermions, gauge bosons or Higgs bosons are favoured. The strength of the coupling depends on k/\bar{M}_{Pl} , where k corresponds to the curvature of the warped extra dimension, and the effective four-dimensional Planck scale $\bar{M}_{Pl} = 2.4 \times 10^{18}$ GeV. The cross section and intrinsic width scale as the square of k/\bar{M}_{Pl} . For the choice $k/\bar{M}_{Pl} = 1$ used in this search, the $\sigma \times \mathcal{B}$ values for $G_{KK} \rightarrow WW$ with W decaying hadronically are 0.54 and 0.026 fb for G_{KK} masses of 2 and 3 TeV, respectively. Corresponding values for $G_{KK} \rightarrow ZZ$ are 0.32 and 0.015 fb. In the

range of G_{KK} masses considered, the branching ratio to WW (ZZ) varies from 24% to 20% (12% to 10%) as the mass increases. Decays into the $t\bar{t}$ final state dominate with a branching ratio varying from 54% to 60%. The G_{KK} resonance has a Γ value that is approximately 6% of its mass.

3. ATLAS detector

The ATLAS experiment [25,26] at the LHC is a multi-purpose particle detector with a forward–backward symmetric cylindrical geometry and a near 4π coverage in solid angle.¹ It consists of an inner detector for tracking surrounded by a thin superconducting solenoid providing a 2 T axial magnetic field, electromagnetic and hadronic calorimeters, and a muon spectrometer. The inner detector covers the pseudorapidity range $|\eta| < 2.5$. It consists of silicon pixel, silicon microstrip, and transition radiation tracking detectors. A new innermost pixel layer [26] inserted at a radius of 3.3 cm has been used since 2015. Lead/liquid-argon (LAr) sampling calorimeters provide electromagnetic (EM) energy measurements with high granularity. A hadronic (steel/scintillator-tile) calorimeter covers the central pseudorapidity range ($|\eta| < 1.7$). The end-cap and forward regions are instrumented with LAr calorimeters for both the EM and hadronic energy measurements up to $|\eta| = 4.9$. The muon spectrometer surrounds the calorimeters and features three large air-core toroidal superconducting magnet systems with eight coils each. The field integral of the toroids ranges between 2.0 and 6.0 Tm across most of the detector. The muon spectrometer includes a system of precision tracking chambers and fast detectors for triggering. A two-level trigger system [27] is used to select events. The first-level trigger is implemented in hardware and uses a subset of the detector information to reduce the accepted rate to at most 100 kHz. This is followed by a software-based trigger level that reduces the accepted event rate to 1 kHz on average.

4. Data and simulation

4.1. Data

The data for this analysis were collected during the LHC pp collision running at $\sqrt{s} = 13$ TeV in 2015 and 2016. Events must pass a trigger-level requirement of having at least one large-radius jet with transverse energy $E_T > 360$ GeV in 2015 and $E_T > 420$ GeV in 2016, where the jet is reconstructed using the anti- k_t algorithm [28] with a radius parameter of 1.0. Those thresholds correspond to the lowest- E_T , unprescaled large-radius jet triggers for each of the two data-taking periods. After requiring that the data were collected during stable beam conditions and the detector components relevant to this analysis were functional, the integrated luminosity of the sample amounts to 3.2 fb⁻¹ and 33.5 fb⁻¹ of pp collisions in 2015 and 2016, respectively.

4.2. Simulation

The search presented here uses simulated Monte Carlo (MC) event samples to optimise the selection criteria, to estimate the

¹ ATLAS uses a right-handed coordinate system with its origin at the nominal interaction point (IP) in the centre of the detector and the z -axis along the beam pipe. The x -axis points from the IP to the centre of the LHC ring, and the y -axis points upwards. Cylindrical coordinates (r, ϕ) are used in the transverse plane, ϕ being the azimuthal angle around the z -axis. The pseudorapidity is defined in terms of the polar angle θ as $\eta = -\ln \tan(\theta/2)$. The rapidity is defined relative to the beam axis as $y = \frac{1}{2} \ln \frac{E+p_z}{E-p_z}$. Angular distance is measured in units of $\Delta R \equiv \sqrt{(\Delta\eta)^2 + (\Delta\phi)^2}$.

acceptance for different signal processes, and to validate the experimental procedure described below. However, it does not rely on MC event samples to estimate the background contribution from SM processes.

Signal events for the heavy scalar model [29] were produced at next-to-leading-order via the gluon–gluon fusion mechanism with POWHEG-Box v1 [30,31] using the CT10 parton distribution function (PDF) set [32]. Events were interfaced with PYTHIA v8.186 [33] for parton showering and hadronisation using the CTEQ6L1 PDF set [34] and the AZNLO set of tuned parameters (later referred to as tune) [35]. The width of the heavy scalar is negligible compared to the experimental resolution.

In the case of the HVT and RS models, events were produced at leading order (LO) with the MADGRAPH5_aMC@NLO v2.2.2 [36] event generator using the NNPDF23LO PDF set [37]. To study the sensitivity of the spin-2 resonance search to production from quark–antiquark or gluon–gluon initial states as well as to different vector-boson polarisation states, events were generated with JHUGen v5.6.3 [38] and the NNPDF23LO PDF set. For these signal models, the event generator was interfaced with PYTHIA v8.186 for parton showering and hadronisation with the A14 tune [39]. The G_{KK} samples are normalised according to calculations from Ref. [40]. In all signal samples, the W and Z bosons are longitudinally polarised.

Multijet background events were generated with PYTHIA v8.186 with the NNPDF23LO PDF set and the A14 tune. Samples of $W +$ jets and $Z +$ jets events were generated with Herwig++ v2.7.1 [41] using the CTEQ6L1 PDF set and the UEEE5 tune [42].

For all MC samples, charm-hadron and bottom-hadron decays were handled by EVTGEN v1.2.0 [43]. Minimum-bias events generated using PYTHIA 8 were added to the hard-scatter interaction in such a way as to reproduce the effects of additional pp interactions in each bunch crossing during data collection (pile-up). An average of 23 pile-up interactions are observed in the data in addition to the hard-scatter interaction. The detector response was simulated with GEANT 4 [44,45] and the events were processed with the same reconstruction software as for the data.

5. Event reconstruction and selection

5.1. Reconstruction

The selection of events relies on the identification and reconstruction of electrons, muons, jets, and missing transverse momentum. Although the analysis primarily relies on jets, other particle candidates are needed to reject events that are included in complementary searches for diboson resonances.

The trajectories of charged particles are reconstructed using measurements in the inner detector. Of the multiple pp collision vertices reconstructed from the available tracks in a given event, a primary vertex is selected as the one with the largest $\sum p_T^2$, where the sum is over all tracks with transverse momentum $p_T > 0.4$ GeV that are associated with the vertex. Tracks that are consistent with the primary vertex may be identified as electron or muon candidates. Electron identification is based on matching tracks to energy clusters in the electromagnetic calorimeter and relying on the longitudinal and transverse shapes of the electromagnetic shower. Electron candidates are required to satisfy the “medium” identification criterion [46] and to pass the “loose” track-based isolation [46]. Muon identification relies on matching tracks in the inner detector to muon spectrometer tracks or track segments. Muon candidates must also satisfy the “medium” selection criterion [47] and the “loose” track isolation [47].

Large-radius jets (hereafter denoted large- R jets) are reconstructed from locally calibrated clusters of energy deposits in

calorimeter cells [48] with the anti- k_t clustering algorithm using a radius parameter $R = 1.0$. Jets are trimmed [49] to minimise the impact of pile-up by reclustering the constituents of each jet with the k_t algorithm [50] into smaller $R = 0.2$ subjets and removing those subjets with $p_T^{\text{subjet}}/p_T^{\text{jet}} < 0.05$, where p_T^{subjet} and p_T^{jet} are the transverse momenta of the subjet and original jet, respectively. The clustering and trimming algorithms use the FastJet package [51]. Calibration of the trimmed jet p_T and mass is described in Ref. [52].

The large- R jet mass is computed using measurements from the calorimeter and tracking systems [53] according to

$$m_J = w^{\text{cal}} m^{\text{cal}} + w^{\text{trk}} \frac{p_T}{p_T^{\text{trk}}} m^{\text{trk}},$$

where p_T^{trk} is the transverse momentum of the jet evaluated using only charged-particle tracks associated with the jet, m^{cal} and m^{trk} are the masses computed using calorimeter and tracker measurements, and w^{cal} and w^{trk} are weights inversely proportional to the square of the resolution of each of the corresponding mass terms. Ghost association [54] is performed to associate tracks to the jets before the trimming procedure is applied. In this method, tracks are added with an infinitesimally small momentum as additional constituents in the jet reconstruction. Tracks associated with the jets are required to have $p_T > 0.4$ GeV and satisfy a number of quality criteria based on the number of measurements in the silicon pixel and microstrip detectors; tracks must also be consistent with originating from the primary vertex [53]. Including information from the tracking system provides improved mass resolution, especially at high jet p_T , due to the relatively coarse angular resolution of the calorimeter.

The magnitude of the event’s missing transverse momentum (E_T^{miss}) is computed from the vectorial sum of calibrated electrons, muons, and jets in the event [55]. For this computation and the rejection of non-collision background discussed below, jets are reconstructed from topological clusters using the anti- k_t algorithm with a radius parameter $R = 0.4$ and are required to satisfy $p_T > 20$ GeV and $|\eta| < 4.9$. Calibration of those jets is described in Ref. [56]. The E_T^{miss} value is corrected using tracks associated with the primary vertex but not associated with electrons, muons or jets.

5.2. Selection

Events used in complementary searches for diboson resonances in different final states are removed, in anticipation of a future combination. Accordingly, events are rejected if they contain any electron or muon with $p_T > 25$ GeV and $|\eta| < 2.5$. Furthermore, events with $E_T^{\text{miss}} > 250$ GeV are rejected.

Events with jets that are likely to be due to non-collision sources, including calorimeter noise, beam halo and cosmic rays, are removed [57]. Events are required to contain at least two large- R jets with $|\eta| < 2.0$ (to guarantee a good overlap with the tracking acceptance) and mass $m_J > 50$ GeV. The leading (highest p_T) large- R jet must have $p_T > 450$ GeV and the subleading (second highest p_T) large- R jet must have $p_T > 200$ GeV. The invariant mass of the dijet system formed by these two jets must be $m_{JJ} > 1.1$ TeV to avoid inefficiencies due to the minimum jet- p_T requirements and to guarantee that the trigger requirement is fully efficient. Only jets in this system are considered in the rest of this Letter. Events passing the above requirements are said to pass the event “preselection”.

Further kinematic requirements are imposed to suppress background from multijet production. The rapidity separation between the leading and subleading jets (identified with subscripts 1 and 2

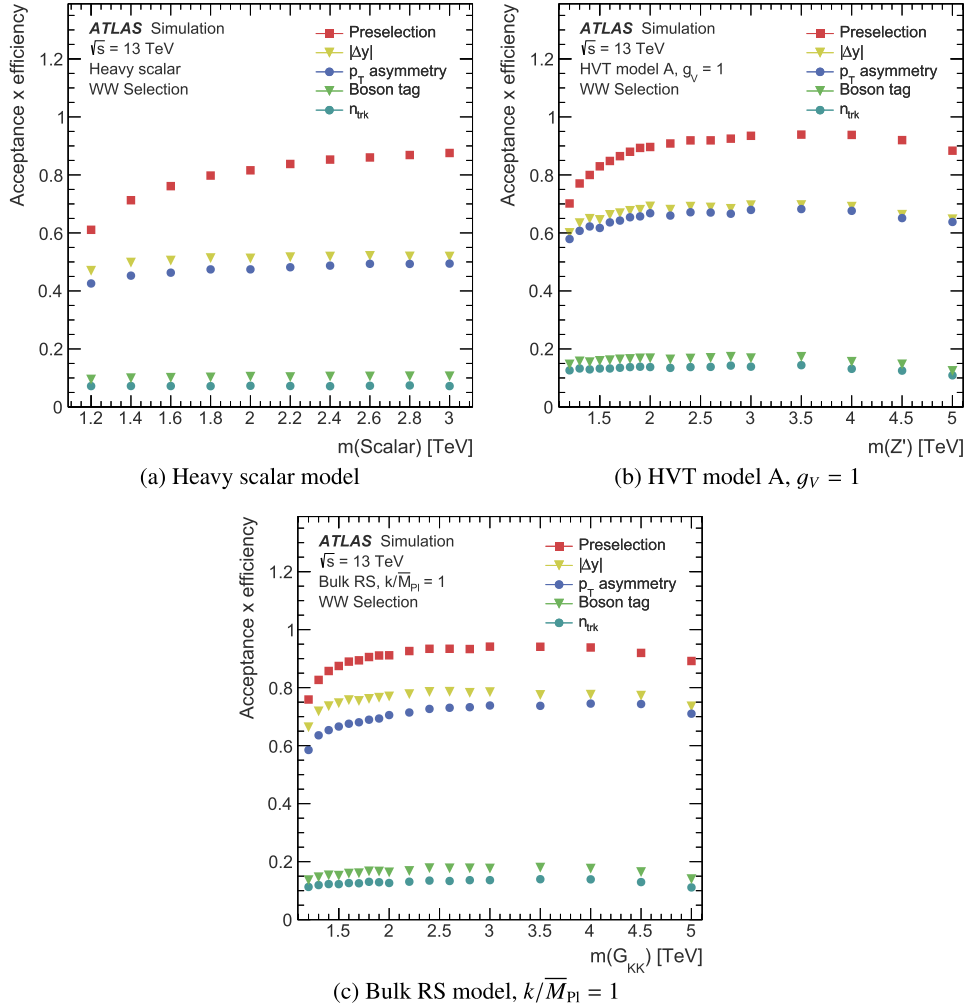


Fig. 1. Signal acceptance times efficiency as a function of resonance mass for (a) $\text{Scalar} \rightarrow WW$ in the heavy scalar model, (b) $Z' \rightarrow WW$ in the HVT model, and (c) $G_{KK} \rightarrow WW$ in the bulk RS model. The acceptance times efficiency is shown at successive stages of selection with the final stage (n_{trk}) corresponding to the signal region.

in the following) must be sufficiently small, $|\Delta y| = |y_1 - y_2| < 1.2$, which is particularly aimed at suppressing t -channel dijet production. The p_T asymmetry between the two jets $A = (p_{T1} - p_{T2}) / (p_{T1} + p_{T2})$ must be smaller than 0.15 to remove events where one jet is poorly reconstructed.

Jets must be consistent with originating from hadronic decays of W or Z bosons. Discrimination against background jets inside a mass window including the W/Z mass is based on the variable D_2 , which is defined as a ratio of two-point to three-point energy correlation functions that are based on the energies of and pairwise angular distances between the jet's constituents [58,59]. This variable is optimised with parameter $\beta = 1$ to distinguish between jets originating from a single parton and those coming from the two-body decay of a heavy particle. A detailed description of the optimisation can be found in Refs. [52,60]. The boson-tagging criteria—the jet-mass window size and maximum D_2 value—are simultaneously optimised to achieve the maximal background-jet rejection for a fixed W or Z signal-jet efficiency of 50%. The optimisation uses signal jets from simulated $W' \rightarrow WZ \rightarrow qq\bar{q}\bar{q}$ events and background jets from simulated multijet events, and depends on the jet p_T to account for varying resolution as a function of jet p_T . The size of the W (Z) mass window varies from 22 (28) GeV near $p_T = 600$ GeV to 40 (40) GeV at $p_T \geq 2500$ GeV and the maximum D_2 value varies from 1.0 to 2.0 as the jet p_T increases. An event is tagged as a candidate WW (ZZ) event if both jets are

within the W (Z) mass window. It can also be tagged as a candidate WZ event if the lower- and higher-mass jets are within the W and Z mass windows, respectively. Because the mass windows are relatively wide and overlap, jets may pass both W - and Z -tagging requirements.

To specifically suppress gluon-initiated jets, the number of tracks associated with each jet must satisfy $n_{\text{trk}} < 30$. The tracks used must have $p_T > 0.5$ GeV and $|\eta| < 2.5$, as well as originate from the primary vertex.

The above set of selection criteria constitutes the signal region (SR) definition. Fig. 1 illustrates the kinematic acceptance times selection efficiency ($\mathcal{A} \times \varepsilon$) at different selection stages for simulated heavy scalar resonances, heavy gauge bosons and KK gravitons decaying to the WW final state. Similar $\mathcal{A} \times \varepsilon$ values are obtained in the WZ final state for the HVT model and in the ZZ final state for the heavy scalar and bulk RS models. Multijet background events are suppressed with a rejection factor of approximately 2×10^5 , as determined from simulation. The figure shows that, among the different selection criteria described above, the boson tagging reduces the signal $\mathcal{A} \times \varepsilon$ the most. However, this particular selection stage provides the most significant suppression of the dominant multijet background.

Table 1 summarises the $\mathcal{A} \times \varepsilon$ values for a number of models at resonance mass values of 2 and 3 TeV for the WW final state; similar results are obtained for the other diboson final states. In

Table 1

Signal acceptance times efficiency for resonances with masses of 2 and 3 TeV decaying into the WW final state in different models. The first three rows correspond to values obtained with the nominal signal MC samples described in Section 4.2 and the values in the last four rows are obtained with the alternate signal MC samples generated with JHUGen.

Model/process	Acceptance \times efficiency	
	$m = 2$ TeV	$m = 3$ TeV
Heavy scalar	7.3%	7.2%
HVT model A, $g_V = 1$	13.8%	13.9%
Bulk RS, $k/\overline{M}_{\text{Pl}} = 1$	12.7%	13.6%
$gg \rightarrow G_{KK} \rightarrow WW$ (longitudinally polarised W)	12.3%	13.4%
$gg \rightarrow G_{KK} \rightarrow WW$ (transversally polarised W)	1.8%	1.9%
$q\bar{q} \rightarrow G_{KK} \rightarrow WW$ (longitudinally polarised W)	5.4%	5.4%
$q\bar{q} \rightarrow G_{KK} \rightarrow WW$ (transversally polarised W)	5.2%	5.8%

the case of the bulk RS model, the KK gravitons are mostly produced via gluon-induced processes and decay into longitudinally polarised W bosons. The polarisation affects the angular separation and momentum sharing between the decay products in the $W \rightarrow qq$ decay and thus affects the boson-tagging efficiency. To test the impact of the polarisation, the $\mathcal{A} \times \varepsilon$ values are evaluated with dedicated signal MC samples initiated by only gluons or quarks, and with W bosons either fully longitudinally polarised or transversely polarised. Significant differences in the signal $\mathcal{A} \times \varepsilon$ are observed, as can be seen in Table 1, and these may need to be taken into account in reinterpretations of the results presented in this Letter. Little dependence is observed on the resonance mass. Differences in $\mathcal{A} \times \varepsilon$ for gluon- and quark-initiated production arise primarily from differences in the acceptance for selection on the jet $|\eta|$ of the two leading jets and their rapidity separation. The boson-tagging efficiency for transversely polarised W bosons is approximately half that for longitudinally polarised W bosons and does not depend appreciably on the heavy-resonance production mechanism. In the case of quark-initiated production, $\mathcal{A} \times \varepsilon$ is similar for longitudinally and transversely polarised W bosons, as the reduction in kinematic acceptance is approximately com-

pensated by an increase in boson-tagging efficiency. In the case of gluon-initiated production, both kinematic acceptance and boson-tagging efficiency favour longitudinally polarised W bosons.

5.3. Validation

In addition to the nominal SR, several validation regions (VRs) are defined to check the analysis procedure and estimate some of the sources of systematic uncertainty.

The definitions of the signal and validation regions are summarised in Table 2. A check of the statistical approach described in Section 6 is performed in the three different sideband validation regions. These correspond to the same selection as for the signal region except for requiring the jet mass to be in one of two sidebands. Both jet masses must be below the W boson mass with $50 < m_j < 60$ –72 GeV (low–low sideband), or above the Z boson mass with 106 –110 < $m_j < 140$ GeV (high–high sideband), or with one jet mass belonging to the low-mass range and the other to the high-mass range (low–high sideband). These mass ranges are chosen to have no overlap with the p_T -dependent W and Z mass windows applied to define the signal regions. The p_T -dependent mass windows imply a range of 60–72 GeV for the upper edge of the lower sideband and 106–110 GeV for the lower edge of the higher sideband.

A $V + \text{jets}$ validation region is defined primarily to compare the observed and simulated $V + \text{jets}$ event yields as a function of the number of tracks associated with the large- R jets and thereby derive an uncertainty in the efficiency for the n_{trk} requirement. There is no attempt at using this validation region to constrain the $V + \text{jets}$ contribution to the signal regions as the total background there is estimated from an empirical fit to the dijet mass distribution. The $V + \text{jets}$ validation region requires the presence of at least two large- R jets with $|\eta| < 2.0$. The leading jet must satisfy $p_T > 600$ GeV and the subleading jet $p_T > 200$ GeV. A higher minimum p_T requirement is imposed on the leading jet than in the nominal event selection to obtain a sample with higher average leading jet p_T that better corresponds to the jet p_T values probed

Table 2

Event selection requirements and definition of the different regions used in the analysis. Different requirements are indicated for the highest- p_T (leading) jet with index 1 and the second highest- p_T (subleading) jet with index 2. The jet mass boundaries applied in the definition of the sideband validation regions depend on the jet p_T .

Signal region	Veto non- $qqqq$ channels: No e or μ with $p_T > 25$ GeV and $ \eta < 2.5$ $E_T^{\text{miss}} < 250$ GeV Event preselection: ≥ 2 large- R jets with $ \eta < 2.0$ and $m_j > 50$ GeV $p_{T1} > 450$ GeV and $p_{T2} > 200$ GeV $m_{jj} > 1.1$ TeV Topology and boson tag: $ \Delta y = y_1 - y_2 < 1.2$ $A = (p_{T1} - p_{T2}) / (p_{T1} + p_{T2}) < 0.15$ Boson tag with D_2 variable and W or Z mass window $n_{\text{trk}} < 30$
Low-low sideband validation region	Same selection as for signal region, except: $50 < m_1 < 60$ –72 GeV and $50 < m_2 < 60$ –72 GeV
High-high sideband validation region	Same selection as for signal region, except: 106 –110 < $m_1 < 140$ GeV and 106 –110 < $m_2 < 140$ GeV
Low-high sideband validation region	Same selection as for signal region, except: $50 < m_1 < 60$ –72 GeV and 106 –110 < $m_2 < 140$ GeV, or 106 –110 < $m_1 < 140$ GeV and $50 < m_2 < 60$ –72 GeV
$V + \text{jets}$ validation region	Veto non- $qqqq$ channels (see above) $V + \text{jets}$ selection: ≥ 2 large- R jets with $ \eta < 2.0$ $p_{T1} > 600$ GeV and $p_{T2} > 200$ GeV Boson tag with D_2 variable only applied to leading jet

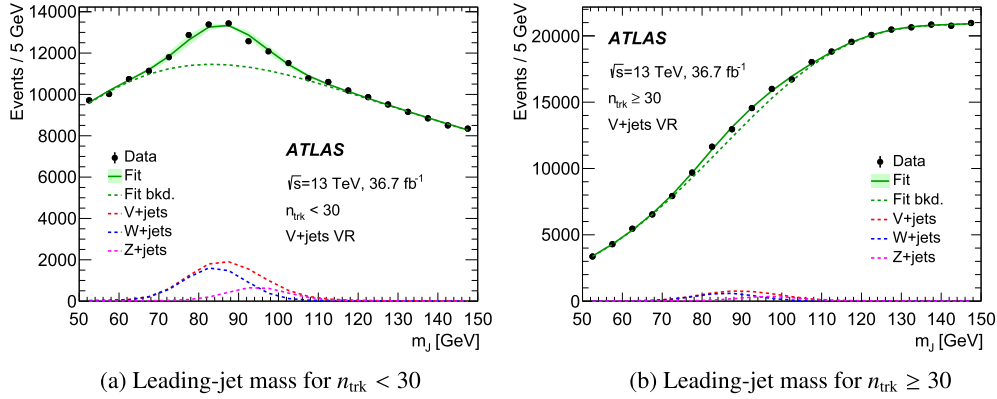


Fig. 2. Leading-jet mass distribution for data in the $V + \text{jets}$ validation region for two different ranges of track multiplicity after boson tagging based only on the D_2 variable. The result of fitting to the sum of functions for the $V + \text{jets}$ and background events is also shown, and described in the text. The error band around the fit result corresponds to the uncertainty in the jet mass scale.

in the search. Finally, the leading jet must pass the boson-tagging requirements based on the D_2 variable only (i.e. the jet mass is not included in the tagging); no boson tagging is applied to the subleading jet. The resulting event sample in this validation region is approximately an order of magnitude larger than the samples selected in the different signal regions. Fig. 2 shows the leading jet mass distribution in the range $50 < m_j < 150$ GeV for events in this $V + \text{jets}$ validation region for $n_{\text{trk}} < 30$ and $n_{\text{trk}} \geq 30$. A clear contribution of W/Z events is visible for $n_{\text{trk}} < 30$ but it is much less apparent for $n_{\text{trk}} \geq 30$, supporting the use of an upper limit on the number of tracks in the signal region.

To establish the efficiency in data of the $n_{\text{trk}} < 30$ selection, the leading-jet mass distribution is analysed in eight multiplicity subsamples, covering $0 \leq n_{\text{trk}} \leq 39$ in groups of five tracks each. Events originating from $W + \text{jets}$ and $Z + \text{jets}$ processes are modelled using a double-Gaussian distribution with the shape parameters determined from simulation, while background events not originating from $V + \text{jets}$ processes are fit to data independently in each subsample using a fourth-order polynomial (denoted “Fit bkd.” in Fig. 2). The relative normalisation in each n_{trk} bin is controlled by a function which has a scaling parameter, allowing a variation in the track efficiency. The relative W and Z boson event contributions are fixed to the prediction from the simulation but the total $W + Z$ event normalisation is determined in the fit. A small upward shift in the W/Z boson peak position is observed as n_{trk} increases, which is well modelled by the simulation. An overall data-to-simulation scale factor of 1.03 ± 0.05 is extracted for the n_{trk} requirement per V jet. As this factor is consistent with unity, no correction is applied.

6. Background parameterisation

The search for diboson resonances is performed by looking for narrow peaks above the smoothly falling m_{jj} distribution expected in the SM. This smoothly falling background mostly consists of SM multijet events. Other SM processes, including diboson, $W/Z + \text{jets}$ and $t\bar{t}$ production, amount to about 15% of the total background. They are also expected to have smoothly falling invariant mass distributions, although not necessarily with the same slope. The background in this search is estimated empirically from a binned maximum-likelihood fit to the observed m_{jj} spectrum in the signal region. The following parametric form is used:

$$\frac{dn}{dx} = p_1(1-x)^{p_2-\xi p_3} x^{-p_3}, \quad (1)$$

where n is the number of events, $x = m_{jj}/\sqrt{s}$, p_1 is a normalisation factor, p_2 and p_3 are dimensionless shape parameters, and ξ is a constant chosen to remove the correlation between p_2 and p_3 in the fit. The latter is determined by repeating the fit with different ξ values. The observed m_{jj} distribution in data is histogrammed with a constant bin size of 100 GeV and the parametric form above is fit in the range $1.1 < m_{jj} < 6.0$ TeV. Only p_2 and p_3 are allowed to vary in the fit since p_1 is fixed by the requirement that the integral of dn/dx equals the number of events in the distribution. This function has been successfully used in previous iterations of this analysis [17]. Other functional forms were tested and no significant improvement in the fit quality was observed.

The ability of the parametric shape in Eq. (1) to model the expected background distribution is tested in the three background-enriched sideband validation regions defined in Table 2. The results of the fits to data are shown in Fig. 3 along with the χ^2 per degree of freedom (DOF). Bins with fewer than five events are grouped with bins that contain at least five events to compute the number of degrees of freedom. The fit model is found to provide a good description of the data in all of the VRs.

A profile likelihood test following Wilks’ theorem [62] is used to determine if including an additional parameter in the background model is necessary. Using the simulated multijet background with the sample size expected for the 2015 + 2016 dataset, as well as large sets of pseudo-experiments, Eq. (1) is found to be sufficient to describe the data. Possible additional uncertainties due to the choice of background model are assessed by performing signal-plus-background fits (also called spurious-signal tests) to the data in the sideband validation regions, where a signal contribution is expected to be negligible. The background is modelled with Eq. (1) and the signal is modelled using resonance mass distributions from simulation. The signal magnitude obtained in these background-dominated regions is less than 25% of its statistical uncertainty at any of the resonance masses considered in this search. Therefore, no additional uncertainty is assigned.

7. Systematic uncertainties

Systematic uncertainties in the signal yield and m_{jj} distribution are assessed, and expressed as additional nuisance parameters in the statistical analysis, as described in Section 8.2. The dominant sources of uncertainty in the signal modelling arise from uncertainties in the large- R jet energy and mass calibrations, affecting the jet p_T , mass and D_2 values. The correlations between the uncertainties in these jet variables are investigated by calculating the resulting uncertainties in the yield at a variety of signal

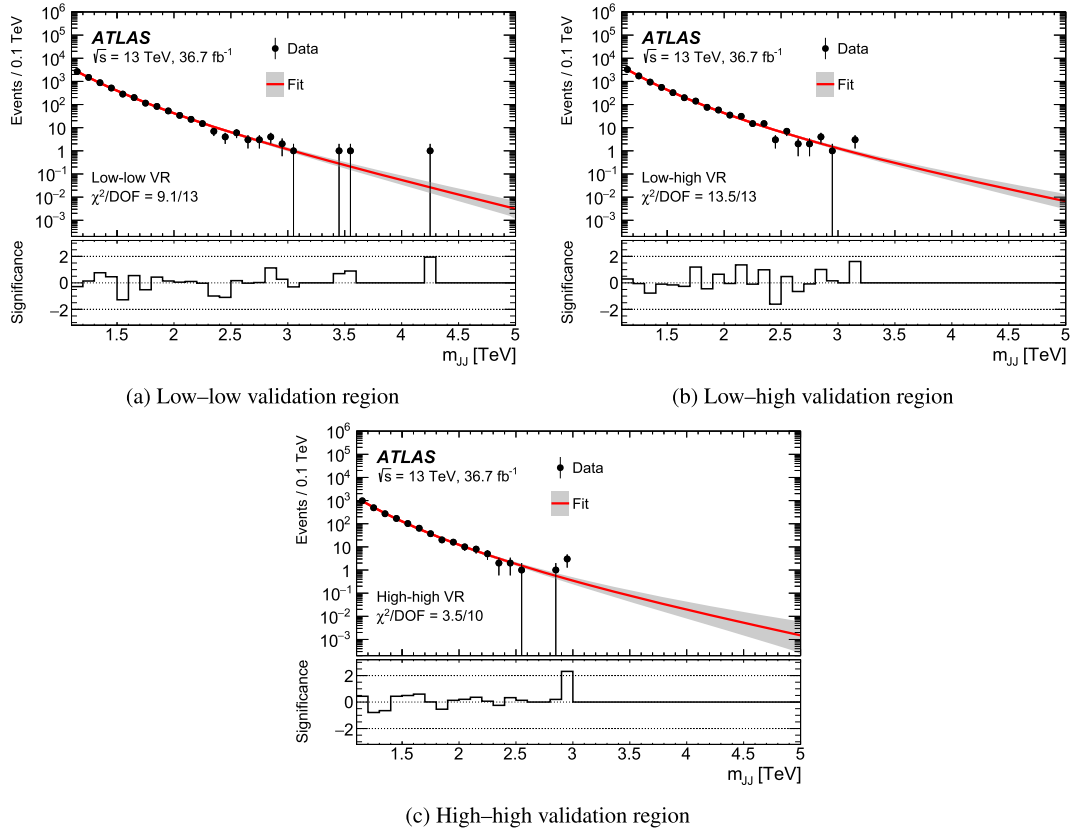


Fig. 3. Dijet mass distributions for data in the sideband validation regions. The solid lines correspond to the result of the fit and the shaded bands represent the uncertainty in the background expectation. The lower panels show the significance of the observed event yield relative to the background fits taking their uncertainties into account as described in Ref. [61].

mass points for three different configurations: “strong”, with all three variables fully correlated; “medium”, with p_T and m_J correlated, whilst the D_2 is uncorrelated; and “weak”, with all three variables fully uncorrelated. The “medium” configuration is chosen as it results in the most conservative (largest) uncertainty in the yield.

Uncertainties in the modelling of the jet energy scale (JES), jet mass scale (JMS) and D_2 scale are evaluated using track-to-calorimeter double ratios between data and MC simulation [63]. This method introduces additional uncertainties from tracking. Uncertainties associated with track reconstruction efficiency, impact parameter resolution, tracking in dense environments, rate for fake tracks and sagitta biases are included. The size of the total correlated JES (JMS) uncertainty varies with jet p_T and is approximately 3% (5%) per jet for the full signal mass range. The uncorrelated scale uncertainty in D_2 also varies with jet p_T and is approximately 3% per jet for the full signal mass range.

Uncertainties in the modelling of jet energy resolution (JER), jet mass resolution (JMR) and D_2 resolution are assessed by applying additional smearing of the jet observables according to the uncertainty in their resolution measurements [52,63]. For the JER a 2% absolute uncertainty is applied per jet, and to mass and D_2 relative uncertainties of 20% and 15% are applied per jet, respectively. The response of the D_2 requirement is not strictly Gaussian and therefore the RMS of the observed distribution is taken as an approximation of the nominal width. There are sufficient dijet data to derive jet-related uncertainties up to jet p_T values of 3 TeV [64].

The efficiency of the $n_{\text{trk}} < 30$ requirement in data and MC simulation is evaluated in the $V + \text{jets}$ VR defined in Section 5.3. The n_{trk} efficiency scale factor is predominantly extracted using jets

with $p_T \approx 650$ GeV, whereas signal jets in the analysis extend to $p_T \geq 1$ TeV. Examining the distribution of the number of tracks associated with jets as a function of jet p_T reveals similar increasing trends in data and MC simulation. However, the average track multiplicity in the simulation is 3% larger at high p_T . Combining the 5% track multiplicity scale uncertainty with the n_{trk} modelling uncertainty leads to a total 6% uncertainty per tagged jet in the efficiency of the n_{trk} requirement. The uncertainty from the trigger selection is found to be negligible, as the minimum requirement on the dijet invariant mass of 1.1 TeV guarantees that the trigger is fully efficient.

Uncertainties affecting the signal prediction are as follows. The uncertainty in the combined 2015 + 2016 integrated luminosity is 3.2%. It is derived, following a methodology similar to that detailed in Ref. [65], from a calibration of the luminosity scale using x - y beam-separation scans performed in August 2015 and May 2016. Theoretical uncertainties in the signal prediction are accounted for via their impact on the signal acceptance. The uncertainty associated with PDFs at high Q^2 values is modelled by taking the envelope formed by the largest deviations produced by the error sets of three PDF sets, as set out by the PDF4LHC group [66]. For the HVT model, the uncertainty ranges from 0.5% to 6% depending on the mass being tested, while a constant 0.5% uncertainty is determined in the case of the heavy scalar and bulk RS models. Uncertainties arising from the choice of A14 tuning parameters are covered by producing samples with variations of the tuning parameters describing initial-state radiation, final-state radiation, and multi-parton interactions. The uncertainty in the signal acceptance is then evaluated at MC generator level, before boson tagging or n_{trk} cuts, resulting in a constant uncertainty of 3% for the HVT model and 5% for the heavy scalar and bulk RS models.

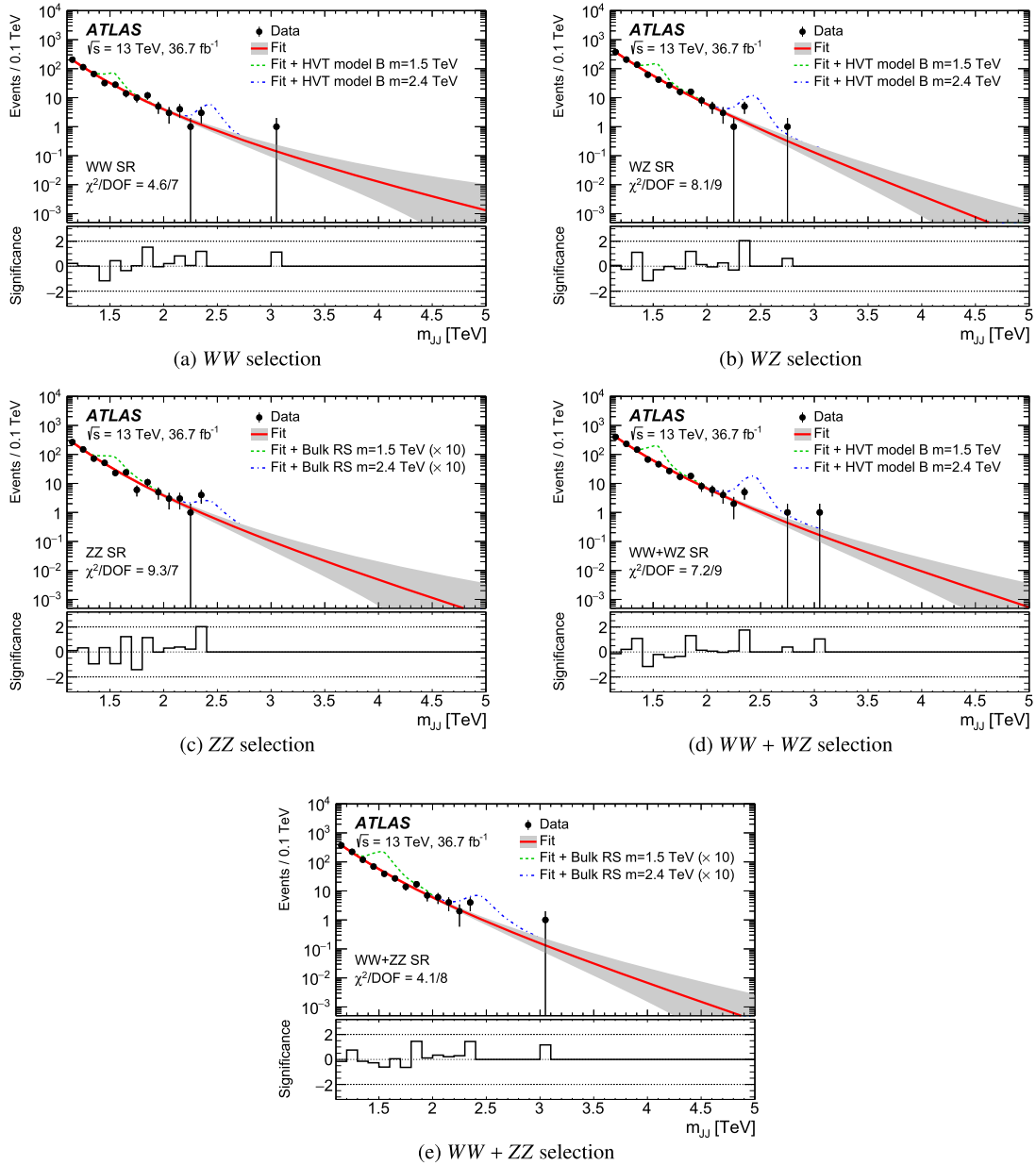


Fig. 4. Dijet mass distributions for data in the (a) WW , (b) WZ , and (c) ZZ signal regions, as well as in the combined (d) $WW + WZ$ and (e) $WW + ZZ$ signal regions. The solid lines correspond to the result of the fit and the shaded bands represent the uncertainty in the background expectation. The lower panels show the significance of the observed event yield relative to the background fits. Expected signals are shown for the HVT model B with $g_V = 3$ and the bulk RS model with $k/\overline{M}_{\text{Pl}} = 1$. The predictions for G_{KK} production are multiplied by a factor of 10. The lower panels show the significance of the observed event yield relative to the background fits taking their uncertainties into account as described in Ref. [61].

8. Results

8.1. Background fit

The fitting procedure described in Section 6 is applied to the data passing the WW , WZ and ZZ selections described in Section 5.2, and resulting dijet mass distributions are shown in Fig. 4. The mass spectra obtained in combined $WW + WZ$ and $WW + ZZ$ SRs are also shown. A total of 497, 904, 618, 980, and 904 events are found in the WW , WZ , ZZ , $WW + WZ$, and $WW + ZZ$ SRs. Approximately 20% of events are included in all three regions: WW , WZ and ZZ . The requirements of the WW (ZZ) SR are satisfied by 47% (57%) of the events in the WZ SR. The fitted background functions shown, labelled “Fit”, are evaluated in bins between 1.1 and 6.0 TeV. No events are observed beyond 3.1 TeV.

The dijet mass distributions in all signal regions are described well by the background model over the whole range explored.

As a test of the background model, the fit is also performed on dijet mass distributions obtained with no boson tagging applied but with weights corresponding to the probability for each jet to satisfy the boson tagging requirements. This probability is derived from the data as a function of the jet p_T and the resulting fits are consistent with the nominal background fits within uncertainties. The use of untagged data allows to validate the model with a sufficiently large number of data events up to dijet masses of 6 TeV.

8.2. Statistical analysis

The final results are interpreted using a frequentist statistical analysis. The parameter of interest is taken to be the signal

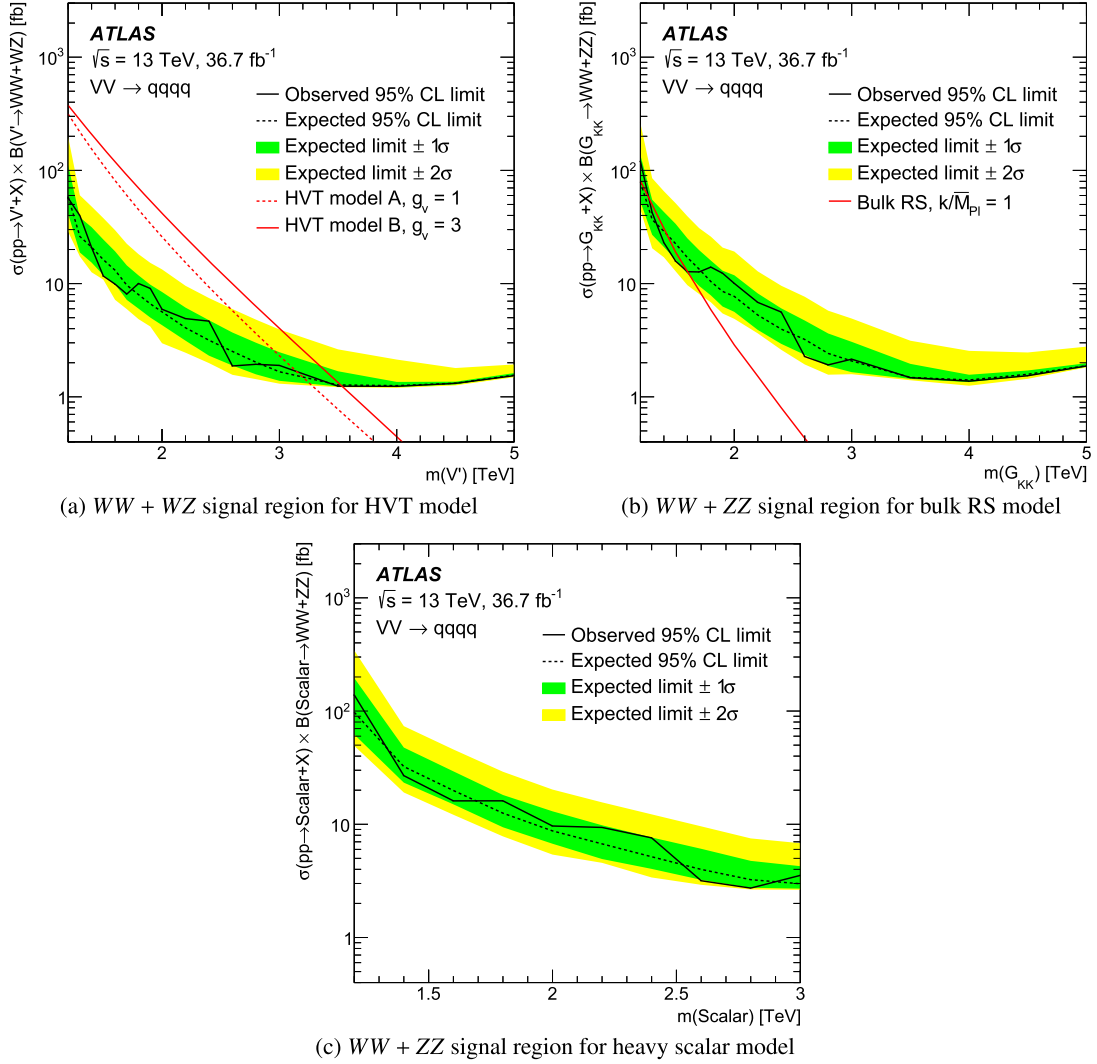


Fig. 5. Upper limits at the 95% CL on the cross section times branching ratio for (a) $WW + WZ$ production as a function of V' mass, (b) $WW + ZZ$ production as a function of G_{KK} mass, and (c) $WW + ZZ$ production as a function of scalar mass. The predicted cross section times branching ratio is shown (a) as dashed and solid lines for the HVT models A with $g_V = 1$ and B with $g_V = 3$, respectively, and (b) as a solid line for the bulk RS model with $k/\bar{M}_{Pl} = 1$.

strength, μ , defined as a scale factor to the number of signal events predicted by the new-physics model being tested. A test statistic $\lambda(\mu)$, based on a profile likelihood ratio [67] is used to extract information about μ from a maximum-likelihood fit of the signal-plus-background model to the data. The likelihood model is defined as

$$\mathcal{L} = \prod_i P_{\text{pois}}(n_{\text{obs}}^i | n_{\text{exp}}^i) \times G(\alpha) \times \mathcal{N}(\theta),$$

where $P_{\text{pois}}(n_{\text{obs}}^i | n_{\text{exp}}^i)$ is the Poisson probability to observe n_{obs}^i events in dijet mass bin i if n_{exp}^i events are expected, $G(\alpha)$ are a series of Gaussian probability density functions modelling the systematic uncertainties, α , related to the shape of the signal, and $\mathcal{N}(\theta)$ is a log-normal distribution for the nuisance parameters, θ , which model the systematic uncertainty in the signal normalisation. The expected number of events is the bin-wise sum of those expected for the signal and background: $n_{\text{exp}} = n_{\text{sig}} + n_{\text{bg}}$. The expected number of background events in bin i , n_{bg}^i , is obtained by integrating dn/dx obtained from Eq. (1) over that bin. Thus, n_{bg} is a function of the background parameters p_1 , p_2 , and p_3 . The number of expected signal events, n_{sig} , is evaluated based on MC simula-

tion assuming the cross section of the model under test multiplied by the signal strength μ .

The significance of any deviation observed in the data with respect to the background-only expectation is quantified in terms of the local p_0 value. This is defined as the probability of fluctuations of the background-only expectation to produce an excess at least as large as the one observed. The largest deviation from the background model occurs in the ZZ SR for a heavy scalar with mass of 2.4 TeV. The local significance of this deviation is 2.0σ and the corresponding global significance is less than 1σ . No statistically significant excess is observed and upper exclusion limits are placed on the cross section times branching ratio for the production of heavy resonances decaying into diboson final states. A correction to account for the branching ratio of V decays into hadronic final states is applied in the results below. The limits are set with the CL_s method [68] using large sets of pseudo-experiments.

Limits on $\sigma \times \mathcal{B}$ are set in each combined diboson channel as a function of the resonance mass. The HVT models A and B with degenerate W' and Z' are used as benchmarks for the combined $WW + WZ$ signal region, and the bulk RS or heavy scalar models are used for the $WW + ZZ$ signal region. Fig. 5(a) shows the observed limits on the production of a spin-1 vector triplet as a func-

Table 3

Observed excluded resonance masses (at 95% CL) in the individual and combined signal regions for the HVT and bulk RS models.

Model	Signal region	Excluded mass range [TeV]
HVT model A, $g_V = 1$	WW	1.20–2.20
	WZ	1.20–3.00
	$WW + WZ$	1.20–3.10
HVT model B, $g_V = 3$	WW	1.20–2.80
	WZ	1.20–3.30
	$WW + WZ$	1.20–3.50
Bulk RS, $k/\overline{M}_{\text{Pl}} = 1$	WW	1.30–1.45
	ZZ	none
	$WW + ZZ$	1.30–1.60

tion of resonance mass in the $WW + WZ$ signal region. A spin-1 vector triplet with couplings predicted by the HVT model A (B) with $g_V = 1$ ($g_V = 3$) is excluded in the range $1.2 < m(V') < 3.1$ ($1.2 < m(V'') < 3.5$) TeV, at the 95% confidence level (CL). Fig. 5(b) shows the observed limits on the production of a G_{KK} as a function of $m(G_{KK})$ in the $WW + ZZ$ signal region. Production of a G_{KK} in the bulk RS model with $k/\overline{M}_{\text{Pl}} = 1$ is excluded in the range $1.3 < m(G_{KK}) < 1.6$ TeV, at the 95% CL. Fig. 5(c) shows the observed limits on the production of a new heavy scalar as a function of $m(\text{Scalar})$ in the $WW + ZZ$ signal region. Table 3 presents the resonance mass ranges excluded at the 95% CL in the various signal regions and signal models considered in the search. In the search for heavy scalar particles, upper limits are set on $\sigma \times \mathcal{B}$ at the 95% CL with values of 9.7 fb at $m(\text{Scalar}) = 2$ TeV and 3.5 fb at $m(\text{Scalar}) = 3$ TeV.

9. Conclusions

This Letter reports a search for massive resonances decaying via WW , WZ and ZZ into hadrons with 36.7 fb^{-1} of $\sqrt{s} = 13$ TeV pp collisions collected at the LHC with the ATLAS detector in 2015–2016. The search takes advantage of the high branching ratio of hadronic decays of the vector bosons and covers the resonance mass range between 1.2 and 5.0 TeV. In this kinematic range, the vector bosons are highly boosted and are reconstructed as single large-radius jets that are tagged by exploiting their two-body substructure. The invariant mass distribution of the two highest- p_T large-radius jets in each event is used to search for narrow resonance peaks over a smoothly falling background. No significant excess of data is observed and limits are set on the cross section times branching ratio for diboson resonances at the 95% confidence level. In the case of the phenomenological HVT model A (model B) with $g_V = 1$ ($g_V = 3$), a spin-1 vector triplet is excluded for masses between 1.2 and 3.1 TeV (1.2 and 3.5 TeV). For the bulk RS model with $k/\overline{M}_{\text{Pl}} = 1$, a spin-2 Kaluza–Klein graviton is excluded in the range between 1.3 and 1.6 TeV. Upper limits on the production cross section times branching ratio for new heavy scalar particles are set with values of 9.7 fb and 3.5 fb at scalar masses of 2 TeV and 3 TeV, respectively.

Acknowledgements

We thank CERN for the very successful operation of the LHC, as well as the support staff from our institutions without whom ATLAS could not be operated efficiently.

We acknowledge the support of ANPCyT, Argentina; YerPhI, Armenia; ARC, Australia; BMWFW and FWF, Austria; ANAS, Azerbaijan; SSTC, Belarus; CNPq and FAPESP, Brazil; NSERC, NRC and CFI, Canada; CERN; CONICYT, Chile; CAS, MOST and NSFC, China; COLCIENCIAS, Colombia; MSMT CR, MPO CR and VSC CR, Czech Republic; DNRF and DNSRC, Denmark; IN2P3-CNRS, CEA-DRF/IRFU,

France; SRNSF, Georgia; BMBF, HGF, and MPG, Germany; GSRT, Greece; RGC, Hong Kong SAR, China; ISF, I-CORE and Benoziyo Center, Israel; INFN, Italy; MEXT and JSPS, Japan; CNRST, Morocco; NWO, Netherlands; RCN, Norway; MNiSW and NCN, Poland; FCT, Portugal; MNE/IFA, Romania; MES of Russia and NRC KI, Russian Federation; JINR; MESTD, Serbia; MSSR, Slovakia; ARRS and MIZŠ, Slovenia; DST/NRF, South Africa; MINECO, Spain; SRC and Wallenberg Foundation, Sweden; SERI, SNSF and Cantons of Bern and Geneva, Switzerland; MOST, Taiwan; TAEK, Turkey; STFC, United Kingdom; DOE and NSF, United States of America. In addition, individual groups and members have received support from BCKDF, the Canada Council, Canarie, CRC, Compute Canada, FQRNT, and the Ontario Innovation Trust, Canada; EPLANET, ERC, ERDF, FP7, Horizon 2020 and Marie Skłodowska-Curie Actions, European Union; Investissements d'Avenir Labex and Idex, ANR, Région Auvergne and Fondation Partager le Savoir, France; DFG and AvH Foundation, Germany; Herakleitos, Thales and Aristeia programmes co-financed by EU-ESF and the Greek NSRF; BSF, GIF and Minerva, Israel; BRF, Norway; CERCA Programme Generalitat de Catalunya, Generalitat Valenciana, Spain; the Royal Society and Leverhulme Trust, United Kingdom.

The crucial computing support from all WLCG partners is acknowledged gratefully, in particular from CERN, the ATLAS Tier-1 facilities at TRIUMF (Canada), NDGF (Denmark, Norway, Sweden), CC-IN2P3 (France), KIT/GridKA (Germany), INFN-CNAF (Italy), NL-T1 (Netherlands), PIC (Spain), ASGC (Taiwan), RAL (UK) and BNL (USA), the Tier-2 facilities worldwide and large non-WLCG resource providers. Major contributors of computing resources are listed in Ref. [69].

References

- [1] G.C. Branco, et al., Theory and phenomenology of two-Higgs-doublet models, *Phys. Rep.* 516 (2012) 1, arXiv:1106.0034 [hep-ph].
- [2] E. Eichten, K. Lane, Low-scale technicolor at the Tevatron and LHC, *Phys. Lett. B* 669 (2008) 235, arXiv:0706.2339 [hep-ph].
- [3] F. Sannino, K. Tuominen, Orientifold theory dynamics and symmetry breaking, *Phys. Rev. D* 71 (2005) 051901, arXiv:hep-ph/0405209.
- [4] J. Andersen, et al., Discovering technicolor, *Eur. Phys. J. Plus* 126 (2011) 81, arXiv:1104.1255 [hep-ph].
- [5] J.C. Pati, A. Salam, Lepton number as the fourth color, *Phys. Rev. D* 10 (1974) 275.
- [6] H. Georgi, S. Glashow, Unity of all elementary particle forces, *Phys. Rev. Lett.* 32 (1974) 438.
- [7] H. Fritzsch, P. Minkowski, Unified interactions of leptons and hadrons, *Ann. Phys.* 93 (1975) 193.
- [8] L. Randall, R. Sundrum, A large mass hierarchy from a small extra dimension, *Phys. Rev. Lett.* 83 (1999) 3370, arXiv:hep-ph/9905221.
- [9] K. Agashe, H. Davoudiasl, G. Perez, A. Soni, Warped gravitons at the LHC and beyond, *Phys. Rev. D* 76 (2007) 036006, arXiv:hep-ph/0701186.
- [10] L. Fitzpatrick, J. Kaplan, L. Randall, L.-T. Wang, Searching for the Kaluza–Klein graviton in bulk RS models, *J. High Energy Phys.* 09 (2007) 013, arXiv:hep-ph/0701150.
- [11] D. Pappadopulo, A. Thamm, R. Torre, A. Wulzer, Heavy vector triplets: bridging theory and data, *J. High Energy Phys.* 09 (2014) 060, arXiv:1402.4431 [hep-ph].
- [12] J. de Blas, J.M. Lizana, M. Perez-Victoria, Combining searches of Z' and W' bosons, *J. High Energy Phys.* 01 (2013) 166, arXiv:1211.2229 [hep-ph].
- [13] ATLAS Collaboration, Search for new phenomena in the $WW \rightarrow \ell\nu\ell'\nu'$ final state in pp collisions at $\sqrt{s} = 7$ TeV with the ATLAS detector, *Phys. Lett. B* 718 (2013) 860, arXiv:1208.2880 [hep-ex].
- [14] ATLAS Collaboration, Search for new particles decaying to ZZ using final states with leptons and jets with the ATLAS detector in $\sqrt{s} = 7$ TeV proton–proton collisions, *Phys. Lett. B* 712 (2012) 331, arXiv:1203.0718 [hep-ex].
- [15] ATLAS Collaboration, Search for WZ resonances in the fully leptonic channel using pp collisions at $\sqrt{s} = 8$ TeV with the ATLAS detector, *Phys. Lett. B* 737 (2014) 223, arXiv:1406.4456 [hep-ex].
- [16] CMS Collaboration, Search for new resonances decaying via WZ to leptons in proton–proton collisions at $\sqrt{s} = 8$ TeV, *Phys. Lett. B* 740 (2015) 83, arXiv:1407.3476 [hep-ex].
- [17] ATLAS Collaboration, Searches for heavy diboson resonances in pp collisions at $\sqrt{s} = 13$ TeV with the ATLAS detector, *J. High Energy Phys.* 09 (2016) 173, arXiv:1606.04833 [hep-ex].

- [18] CMS Collaboration, Search for massive resonances decaying into pairs of boosted bosons in semi-leptonic final states at $\sqrt{s} = 8$ TeV, *J. High Energy Phys.* 08 (2014) 174, arXiv:1405.3447 [hep-ex].
- [19] CMS Collaboration, Search for massive resonances decaying into WW , WZ or ZZ bosons in proton–proton collisions at $\sqrt{s} = 13$ TeV, *J. High Energy Phys.* 03 (2017) 162, arXiv:1612.09159 [hep-ex].
- [20] J.M. Cornwall, D.N. Levin, G. Tiktopoulos, Derivation of gauge invariance from high-energy unitarity bounds on the S matrix, *Phys. Rev. D* 10 (1974) 1145; Erratum: *Phys. Rev. D* 11 (1975) 972.
- [21] G.J. Gounaris, R. Kogerler, H. Neufeld, Relationship between longitudinally polarized vector bosons and their unphysical scalar partners, *Phys. Rev. D* 34 (1986) 3257.
- [22] M.S. Chanowitz, M.K. Gaillard, The TeV physics of strongly interacting W 's and Z 's, *Nucl. Phys. B* 261 (1985) 379.
- [23] ATLAS Collaboration, Search for new high-mass phenomena in the dilepton final state using 36.1 fb^{-1} of proton–proton collision data at $\sqrt{s} = 13$ TeV with the ATLAS detector, *J. High Energy Phys.* 10 (2017) 182, arXiv:1707.02424 [hep-ex].
- [24] ATLAS Collaboration, Search for a new heavy gauge boson resonance decaying into a lepton and missing transverse momentum in 36 fb^{-1} of pp collisions at $\sqrt{s} = 13$ TeV with the ATLAS experiment, arXiv:1706.04786 [hep-ex], 2017.
- [25] ATLAS Collaboration, The ATLAS experiment at the CERN Large Hadron Collider, *J. Instrum.* 3 (2008) S08003.
- [26] ATLAS Collaboration, ATLAS Insertable B-Layer Technical Design Report, ATLAS-TDR-19, 2010, <https://cds.cern.ch/record/1291633>; ATLAS Collaboration, ATLAS Insertable B-Layer Technical Design Report Addendum, ATLAS-TDR-19-ADD-1, 2012, <https://cds.cern.ch/record/1451888>.
- [27] ATLAS Collaboration, Performance of the ATLAS trigger system in 2015, *Eur. Phys. J. C* 77 (2017) 317, arXiv:1611.09661 [hep-ex].
- [28] M. Cacciari, G.P. Salam, G. Soyez, The anti- k_t jet clustering algorithm, *J. High Energy Phys.* 04 (2008) 063, arXiv:0802.1189 [hep-ph].
- [29] V. Barger, P. Langacker, M. McCaskey, M.J. Ramsey-Musolf, G. Shaughnessy, LHC phenomenology of an extended Standard Model with a real scalar singlet, *Phys. Rev. D* 77 (2008) 035005, arXiv:0706.4311 [hep-ph].
- [30] S. Alioli, P. Nason, C. Oleari, E. Re, A general framework for implementing NLO calculations in shower Monte Carlo programs: the POWHEG BOX, *J. High Energy Phys.* 06 (2010) 043, arXiv:1002.2581 [hep-ph].
- [31] S. Alioli, P. Nason, C. Oleari, E. Re, NLO Higgs boson production via gluon fusion matched with shower in POWHEG, *J. High Energy Phys.* 04 (2009) 002, arXiv:0812.0578 [hep-ph].
- [32] H.-L. Lai, et al., New parton distributions for collider physics, *Phys. Rev. D* 82 (2010) 074024, arXiv:1007.2241 [hep-ph].
- [33] T. Sjöstrand, S. Mrenna, P.Z. Skands, A brief introduction to PYTHIA 8.1, *Comput. Phys. Commun.* 178 (2008) 852, arXiv:0710.3820 [hep-ph].
- [34] J. Pumplin, et al., New generation of parton distributions with uncertainties from global QCD analysis, *J. High Energy Phys.* 07 (2002) 012, arXiv:hep-ph/0201195.
- [35] ATLAS Collaboration, Measurement of the Z/γ^* boson transverse momentum distribution in pp collisions at $\sqrt{s} = 7$ TeV with the ATLAS detector, *J. High Energy Phys.* 09 (2014) 145, arXiv:1406.3660 [hep-ex].
- [36] J. Alwall, et al., The automated computation of tree-level and next-to-leading order differential cross sections, and their matching to parton shower simulations, *J. High Energy Phys.* 07 (2014) 079, arXiv:1405.0301 [hep-ph].
- [37] R.D. Ball, et al., Parton distributions with LHC data, *Nucl. Phys. B* 867 (2013) 244, arXiv:1207.1303 [hep-ph].
- [38] Y. Gao, et al., Spin determination of single-produced resonances at hadron colliders, *Phys. Rev. D* 81 (2010) 075022, arXiv:1001.3396 [hep-ph].
- [39] ATLAS Collaboration, ATLAS Pythia 8 Tunes to 7 TeV Data, ATL-PHYS-PUB-2014-021, 2014, <https://cds.cern.ch/record/1966419>.
- [40] A. Oliveira, Gravity particles from warped extra dimensions, predictions for LHC, arXiv:1404.0102 [hep-ph], 2014.
- [41] M. Bahr, et al., Herwig++ physics and manual, *Eur. Phys. J. C* 58 (2008) 639, arXiv:0803.0883 [hep-ph].
- [42] S. Gieseke, C. Rohr, A. Siodmok, Colour reconnections in Herwig++, *Eur. Phys. J. C* 72 (2012) 2225, arXiv:1206.0041 [hep-ph].
- [43] D.J. Lange, The EvtGen particle decay simulation package, *Nucl. Instrum. Methods A* 462 (2001) 152.
- [44] S. Agostinelli, et al., GEANT4 – a simulation toolkit, *Nucl. Instrum. Methods A* 506 (2003) 250.
- [45] ATLAS Collaboration, The ATLAS simulation infrastructure, *Eur. Phys. J. C* 70 (2010) 823, arXiv:1005.4568 [physics.ins-det].
- [46] ATLAS Collaboration, Electron Efficiency Measurements with the ATLAS Detector Using the 2015 LHC Proton–Proton Collision Data, ATLAS-CONF-2016-024, 2016, <https://cds.cern.ch/record/2157687>.
- [47] ATLAS Collaboration, Muon reconstruction performance of the ATLAS detector in proton–proton collision data at $\sqrt{s} = 13$ TeV, *Eur. Phys. J. C* 76 (2016) 292, arXiv:1603.05598 [hep-ex].
- [48] ATLAS Collaboration, Jet energy measurement with the ATLAS detector in proton–proton collisions at $\sqrt{s} = 7$ TeV, *Eur. Phys. J. C* 73 (2013) 2304, arXiv:1112.6426 [hep-ex].
- [49] D. Krohn, J. Thaler, L.-T. Wang, Jet trimming, *J. High Energy Phys.* 02 (2010) 084, arXiv:0912.1342 [hep-ph].
- [50] S.D. Ellis, D.E. Soper, Successive combination jet algorithm for hadron collisions, *Phys. Rev. D* 48 (1993) 3160, arXiv:hep-ph/9305266.
- [51] M. Cacciari, G.P. Salam, G. Soyez, FastJet user manual, *Eur. Phys. J. C* 72 (2012) 1896, arXiv:1111.6097 [hep-ph].
- [52] ATLAS Collaboration, Identification of Boosted, Hadronically-Decaying W and Z Bosons in $\sqrt{s} = 13$ TeV Monte Carlo Simulations for ATLAS, ATL-PHYS-PUB-2015-033, 2015, <https://cds.cern.ch/record/2041461>.
- [53] ATLAS Collaboration, Jet Mass Reconstruction with the ATLAS Detector in Early Run 2 Data, ATLAS-CONF-2016-035, 2016, <https://cds.cern.ch/record/2200211>.
- [54] M. Cacciari, G.P. Salam, Pileup subtraction using jet areas, *Phys. Lett. B* 659 (2008) 119, arXiv:0707.1378 [hep-ph].
- [55] ATLAS Collaboration, Performance of algorithms that reconstruct missing transverse momentum in $\sqrt{s} = 8$ TeV proton–proton collisions in the ATLAS detector, *Eur. Phys. J. C* 77 (2017) 241, arXiv:1609.09324 [hep-ex].
- [56] ATLAS Collaboration, Jet energy scale measurements and their systematic uncertainties in proton–proton collisions at $\sqrt{s} = 13$ TeV with the ATLAS detector, *Phys. Rev. D* 96 (2017) 072002, arXiv:1703.09665 [hep-ex].
- [57] ATLAS Collaboration, Selection of Jets Produced in 13 TeV Proton–Proton Collisions with the ATLAS Detector, ATLAS-CONF-2015-029, 2015, <https://cds.cern.ch/record/2037702>.
- [58] A.J. Larkoski, I. Moult, D. Neill, Power counting to better jet observables, *J. High Energy Phys.* 12 (2014) 009, arXiv:1409.6298 [hep-ph].
- [59] A.J. Larkoski, I. Moult, D. Neill, Analytic boosted boson discrimination, *J. High Energy Phys.* 05 (2016) 117, arXiv:1507.03018 [hep-ph].
- [60] ATLAS Collaboration, Identification of boosted, hadronically decaying W bosons and comparisons with ATLAS data taken at $\sqrt{s} = 8$ TeV, *Eur. Phys. J. C* 76 (2016) 154, arXiv:1510.05821 [hep-ex].
- [61] G. Choudalakis, D. Casadei, Plotting the differences between data and expectation, *Eur. Phys. J. Plus* 127 (2012) 25, arXiv:1111.2062 [physics.data-an].
- [62] S.S. Wilks, The large-sample distribution of the likelihood ratio for testing composite hypotheses, *Ann. Math. Stat.* 9 (1938) 60.
- [63] ATLAS Collaboration, Performance of jet substructure techniques for large- R jets in proton–proton collisions at $\sqrt{s} = 7$ TeV using the ATLAS detector, *J. High Energy Phys.* 09 (2013) 076, arXiv:1306.4945 [hep-ex].
- [64] ATLAS Collaboration, In-situ Measurements of the ATLAS Large-Radius Jet Response in 13 TeV pp Collisions, ATLAS-CONF-2017-063, 2017, <https://cds.cern.ch/record/2275655>.
- [65] ATLAS Collaboration, Luminosity determination in pp collisions at $\sqrt{s} = 8$ TeV using the ATLAS detector at the LHC, *Eur. Phys. J. C* 76 (2016) 653, arXiv:1608.03953 [hep-ex].
- [66] J. Butterworth, et al., PDF4LHC recommendations for LHC Run II, *J. Phys. G* 43 (2016) 023001, arXiv:1510.03865 [hep-ph].
- [67] G. Cowan, K. Cranmer, E. Gross, O. Vitells, Asymptotic formulae for likelihood-based tests of new physics, *Eur. Phys. J. C* 71 (2011) 1554, arXiv:1007.1727 [physics.data-an]; Erratum: *Eur. Phys. J. C* 73 (2013) 2501.
- [68] A.L. Read, Presentation of search results: the CL_s technique, *J. Phys. G* 28 (2002) 2693.
- [69] ATLAS Collaboration, ATLAS Computing Acknowledgements 2016–2017, ATL-GEN-PUB-2016-002, <https://cds.cern.ch/record/2202407>.

The ATLAS Collaboration

M. Aaboud^{137d}, G. Aad⁸⁸, B. Abbott¹¹⁵, O. Abdinov^{12,*}, B. Abeloos¹¹⁹, S.H. Abidi¹⁶¹, O.S. AbouZeid¹³⁹, N.L. Abraham¹⁵¹, H. Abramowicz¹⁵⁵, H. Abreu¹⁵⁴, R. Abreu¹¹⁸, Y. Abulaiti^{148a,148b}, B.S. Acharya^{167a,167b,a}, S. Adachi¹⁵⁷, L. Adamczyk^{41a}, J. Adelman¹¹⁰, M. Adersberger¹⁰², T. Adye¹³³, A.A. Affolder¹³⁹, Y. Afik¹⁵⁴, T. Agatonovic-Jovin¹⁴, C. Agheorghiesei^{28c}, J.A. Aguilar-Saavedra^{128a,128f},

S.P. Ahlen²⁴, F. Ahmadov^{68,b}, G. Aielli^{135a,135b}, S. Akatsuka⁷¹, H. Akerstedt^{148a,148b}, T.P.A. Åkesson⁸⁴, E. Akilli⁵², A.V. Akimov⁹⁸, G.L. Alberghi^{22a,22b}, J. Albert¹⁷², P. Albicocco⁵⁰, M.J. Alconada Verzini⁷⁴, S.C. Alderweireldt¹⁰⁸, M. Aleksa³², I.N. Aleksandrov⁶⁸, C. Alexa^{28b}, G. Alexander¹⁵⁵, T. Alexopoulos¹⁰, M. Alhroob¹¹⁵, B. Ali¹³⁰, M. Aliev^{76a,76b}, G. Alimonti^{94a}, J. Alison³³, S.P. Alkire³⁸, B.M.M. Allbrooke¹⁵¹, B.W. Allen¹¹⁸, P.P. Allport¹⁹, A. Aloisio^{106a,106b}, A. Alonso³⁹, F. Alonso⁷⁴, C. Alpigiani¹⁴⁰, A.A. Alshehri⁵⁶, M.I. Alstamy⁸⁸, B. Alvarez Gonzalez³², D. Álvarez Piqueras¹⁷⁰, M.G. Alvigi^{106a,106b}, B.T. Amadio¹⁶, Y. Amaral Coutinho^{26a}, C. Amelung²⁵, D. Amidei⁹², S.P. Amor Dos Santos^{128a,128c}, S. Amoroso³², G. Amundsen²⁵, C. Anastopoulos¹⁴¹, L.S. Ancu⁵², N. Andari¹⁹, T. Andeen¹¹, C.F. Anders^{60b}, J.K. Anders⁷⁷, K.J. Anderson³³, A. Andreazza^{94a,94b}, V. Andrei^{60a}, S. Angelidakis³⁷, I. Angelozzi¹⁰⁹, A. Angerami³⁸, A.V. Anisenkov^{111,c}, N. Anjos¹³, A. Annovi^{126a,126b}, C. Antel^{60a}, M. Antonelli⁵⁰, A. Antonov^{100,*}, D.J. Antrim¹⁶⁶, F. Anulli^{134a}, M. Aoki⁶⁹, L. Aperio Bella³², G. Arabidze⁹³, Y. Arai⁶⁹, J.P. Araque^{128a}, V. Araujo Ferraz^{26a}, A.T.H. Arce⁴⁸, R.E. Ardell⁸⁰, F.A. Arduh⁷⁴, J.-F. Arguin⁹⁷, S. Argyropoulos⁶⁶, M. Arik^{20a}, A.J. Armbruster³², L.J. Armitage⁷⁹, O. Arnaez¹⁶¹, H. Arnold⁵¹, M. Arratia³⁰, O. Arslan²³, A. Artamonov^{99,*}, G. Artoni¹²², S. Artz⁸⁶, S. Asai¹⁵⁷, N. Asbah⁴⁵, A. Ashkenazi¹⁵⁵, L. Asquith¹⁵¹, K. Assamagan²⁷, R. Astalos^{146a}, M. Atkinson¹⁶⁹, N.B. Atlay¹⁴³, K. Augsten¹³⁰, G. Avolio³², B. Axen¹⁶, M.K. Ayoub^{35a}, G. Azuelos^{97,d}, A.E. Baas^{60a}, M.J. Baca¹⁹, H. Bachacou¹³⁸, K. Bachas^{76a,76b}, M. Backes¹²², P. Bagnaia^{134a,134b}, M. Bahmani⁴², H. Bahrasemani¹⁴⁴, J.T. Baines¹³³, M. Bajic³⁹, O.K. Baker¹⁷⁹, P.J. Bakker¹⁰⁹, E.M. Baldin^{111,c}, P. Balek¹⁷⁵, F. Balli¹³⁸, W.K. Balunas¹²⁴, E. Banas⁴², A. Bandyopadhyay²³, Sw. Banerjee^{176,e}, A.A.E. Bannoura¹⁷⁸, L. Barak¹⁵⁵, E.L. Barberio⁹¹, D. Barberis^{53a,53b}, M. Barbero⁸⁸, T. Barillari¹⁰³, M.-S. Barisits³², J.T. Barkeloo¹¹⁸, T. Barklow¹⁴⁵, N. Barlow³⁰, S.L. Barnes^{36c}, B.M. Barnett¹³³, R.M. Barnett¹⁶, Z. Barnovska-Blenessy^{36a}, A. Baroncelli^{136a}, G. Barone²⁵, A.J. Barr¹²², L. Barranco Navarro¹⁷⁰, F. Barreiro⁸⁵, J. Barreiro Guimarães da Costa^{35a}, R. Bartoldus¹⁴⁵, A.E. Barton⁷⁵, P. Bartos^{146a}, A. Basalae¹²⁵, A. Bassalat^{119,f}, R.L. Bates⁵⁶, S.J. Batista¹⁶¹, J.R. Batley³⁰, M. Battaglia¹³⁹, M. Baue^{134a,134b}, F. Bauer¹³⁸, H.S. Bawa^{145,g}, J.B. Beacham¹¹³, M.D. Beattie⁷⁵, T. Beau⁸³, P.H. Beauchemin¹⁶⁵, P. Bechtel²³, H.P. Beck^{18,h}, H.C. Beck⁵⁷, K. Becker¹²², M. Becker⁸⁶, C. Becot¹¹², A.J. Beddall^{20e}, A. Beddall^{20b}, V.A. Bednyakov⁶⁸, M. Bedognetti¹⁰⁹, C.P. Bee¹⁵⁰, T.A. Beermann³², M. Begalli^{26a}, M. Begel²⁷, J.K. Behr⁴⁵, A.S. Bell⁸¹, G. Bella¹⁵⁵, L. Bellagamba^{22a}, A. Bellerive³¹, M. Bellomo¹⁵⁴, K. Belotskiy¹⁰⁰, O. Beltramello³², N.L. Belyaev¹⁰⁰, O. Benary^{155,*}, D. Benchechroun^{137a}, M. Bender¹⁰², N. Benekos¹⁰, Y. Benhammou¹⁵⁵, E. Benhar Noccioli¹⁷⁹, J. Benitez⁶⁶, D.P. Benjamin⁴⁸, M. Benoit⁵², J.R. Bensinger²⁵, S. Bentvelsen¹⁰⁹, L. Beresford¹²², M. Beretta⁵⁰, D. Berge¹⁰⁹, E. Bergeaas Kuutmann¹⁶⁸, N. Berger⁵, J. Beringer¹⁶, S. Berlendis⁵⁸, N.R. Bernard⁸⁹, G. Bernardi⁸³, C. Bernius¹⁴⁵, F.U. Bernlochner²³, T. Berry⁸⁰, P. Berta⁸⁶, C. Bertella^{35a}, G. Bertoli^{148a,148b}, I.A. Bertram⁷⁵, C. Bertsche⁴⁵, D. Bertsche¹¹⁵, G.J. Besjes³⁹, O. Bessidskaia Bylund^{148a,148b}, M. Bessner⁴⁵, N. Besson¹³⁸, A. Bethani⁸⁷, S. Bethke¹⁰³, A. Betti²³, A.J. Bevan⁷⁹, J. Beyer¹⁰³, R.M. Bianchi¹²⁷, O. Biebel¹⁰², D. Biedermann¹⁷, R. Bielski⁸⁷, K. Bierwagen⁸⁶, N.V. Biesuz^{126a,126b}, M. Biglietti^{136a}, T.R.V. Billoud⁹⁷, H. Bilokon⁵⁰, M. Bindi⁵⁷, A. Bingul^{20b}, C. Bini^{134a,134b}, S. Biondi^{22a,22b}, T. Bisanz⁵⁷, C. Bittrich⁴⁷, D.M. Bjergaard⁴⁸, J.E. Black¹⁴⁵, K.M. Black²⁴, R.E. Blair⁶, T. Blazek^{146a}, I. Bloch⁴⁵, C. Blocker²⁵, A. Blue⁵⁶, W. Blum^{86,*}, U. Blumenschein⁷⁹, S. Blunier^{34a}, G.J. Bobbink¹⁰⁹, V.S. Bobrovnikov^{111,c}, S.S. Bocchetta⁸⁴, A. Bocci⁴⁸, C. Bock¹⁰², M. Boehler⁵¹, D. Boerner¹⁷⁸, D. Bogavac¹⁰², A.G. Bogdanchikov¹¹¹, C. Böhm^{148a}, V. Boisvert⁸⁰, P. Bokan^{168,i}, T. Bold^{41a}, A.S. Boldyrev¹⁰¹, A.E. Bolz^{60b}, M. Bomben⁸³, M. Bona⁷⁹, M. Boonekamp¹³⁸, A. Borisov¹³², G. Borissov⁷⁵, J. Bortfeldt³², D. Bortoletto¹²², V. Bortolotto^{62a}, D. Boscherini^{22a}, M. Bosman¹³, J.D. Bossio Sola²⁹, J. Boudreau¹²⁷, J. Bouffard², E.V. Bouhova-Thacker⁷⁵, D. Boumediene³⁷, C. Bourdarios¹¹⁹, S.K. Boutle⁵⁶, A. Boveia¹¹³, J. Boyd³², I.R. Boyko⁶⁸, A.J. Bozson⁸⁰, J. Bracinik¹⁹, A. Brandt⁸, G. Brandt⁵⁷, O. Brandt^{60a}, F. Braren⁴⁵, U. Bratzler¹⁵⁸, B. Brau⁸⁹, J.E. Brau¹¹⁸, W.D. Breaden Madden⁵⁶, K. Brendlinger⁴⁵, A.J. Brennan⁹¹, L. Brenner¹⁰⁹, R. Brenner¹⁶⁸, S. Bressler¹⁷⁵, D.L. Briglin¹⁹, T.M. Bristow⁴⁹, D. Britton⁵⁶, D. Britzger⁴⁵, F.M. Brochu³⁰, I. Brock²³, R. Brock⁹³, G. Brooijmans³⁸, T. Brooks⁸⁰, W.K. Brooks^{34b}, J. Brosamer¹⁶, E. Brost¹¹⁰, J.H. Broughton¹⁹, P.A. Bruckman de Renstrom⁴², D. Bruncko^{146b}, A. Bruni^{22a}, G. Bruni^{22a}, L.S. Bruni¹⁰⁹, S. Bruno^{135a,135b}, B.H. Brunt³⁰, M. Bruschi^{22a}, N. Bruscino¹²⁷, P. Bryant³³, L. Bryngemark⁴⁵, T. Buanes¹⁵, Q. Buat¹⁴⁴, P. Buchholz¹⁴³, A.G. Buckley⁵⁶, I.A. Budagov⁶⁸, F. Buehrer⁵¹, M.K. Bugge¹²¹, O. Bulekov¹⁰⁰, D. Bullock⁸, T.J. Burch¹¹⁰, S. Burdin⁷⁷, C.D. Burgard⁵¹, A.M. Burger⁵, B. Burghgrave¹¹⁰, K. Burka⁴², S. Burke¹³³,

I. Burmeister⁴⁶, J.T.P. Burr¹²², E. Busato³⁷, D. Büscher⁵¹, V. Büscher⁸⁶, P. Bussey⁵⁶, J.M. Butler²⁴, C.M. Buttar⁵⁶, J.M. Butterworth⁸¹, P. Butti³², W. Buttinger²⁷, A. Buzatu¹⁵³, A.R. Buzykaev^{111,c}, S. Cabrera Urbán¹⁷⁰, D. Caforio¹³⁰, H. Cai¹⁶⁹, V.M. Cairo^{40a,40b}, O. Cakir^{4a}, N. Calace⁵², P. Calafiura¹⁶, A. Calandri⁸⁸, G. Calderini⁸³, P. Calfayan⁶⁴, G. Callea^{40a,40b}, L.P. Caloba^{26a}, S. Calvente Lopez⁸⁵, D. Calvet³⁷, S. Calvet³⁷, T.P. Calvet⁸⁸, R. Camacho Toro³³, S. Camarda³², P. Camarri^{135a,135b}, D. Cameron¹²¹, R. Caminal Armadans¹⁶⁹, C. Camincher⁵⁸, S. Campana³², M. Campanelli⁸¹, A. Camplani^{94a,94b}, A. Campoverde¹⁴³, V. Canale^{106a,106b}, M. Cano Bret^{36c}, J. Cantero¹¹⁶, T. Cao¹⁵⁵, M.D.M. Capeans Garrido³², I. Caprini^{28b}, M. Caprini^{28b}, M. Capua^{40a,40b}, R.M. Carbone³⁸, R. Cardarelli^{135a}, F. Cardillo⁵¹, I. Carli¹³¹, T. Carli³², G. Carlino^{106a}, B.T. Carlson¹²⁷, L. Carminati^{94a,94b}, R.M.D. Carney^{148a,148b}, S. Caron¹⁰⁸, E. Carquin^{34b}, S. Carrá^{94a,94b}, G.D. Carrillo-Montoya³², D. Casadei¹⁹, M.P. Casado^{13,j}, M. Casolino¹³, D.W. Casper¹⁶⁶, R. Castelijin¹⁰⁹, V. Castillo Gimenez¹⁷⁰, N.F. Castro^{128a,k}, A. Catinaccio³², J.R. Catmore¹²¹, A. Cattai³², J. Caudron²³, V. Cavaliere¹⁶⁹, E. Cavallaro¹³, D. Cavalli^{94a}, M. Cavalli-Sforza¹³, V. Cavasinni^{126a,126b}, E. Celebi^{20d}, F. Ceradini^{136a,136b}, L. Cerda Alberich¹⁷⁰, A.S. Cerqueira^{26b}, A. Cerri¹⁵¹, L. Cerrito^{135a,135b}, F. Cerutti¹⁶, A. Cervelli^{22a,22b}, S.A. Cetin^{20d}, A. Chafaq^{137a}, D. Chakraborty¹¹⁰, S.K. Chan⁵⁹, W.S. Chan¹⁰⁹, Y.L. Chan^{62a}, P. Chang¹⁶⁹, J.D. Chapman³⁰, D.G. Charlton¹⁹, C.C. Chau³¹, C.A. Chavez Barajas¹⁵¹, S. Che¹¹³, S. Cheatham^{167a,167c}, A. Chegwidden⁹³, S. Chekanov⁶, S.V. Chekulaev^{163a}, G.A. Chelkov^{68,l}, M.A. Chelstowska³², C. Chen^{36a}, C. Chen⁶⁷, H. Chen²⁷, J. Chen^{36a}, S. Chen^{35b}, S. Chen¹⁵⁷, X. Chen^{35c,m}, Y. Chen⁷⁰, H.C. Cheng⁹², H.J. Cheng^{35a}, A. Cheplakov⁶⁸, E. Cheremushkina¹³², R. Cherkouli El Moursli^{137e}, E. Cheu⁷, K. Cheung⁶³, L. Chevalier¹³⁸, V. Chiarella⁵⁰, G. Chiarelli^{126a,126b}, G. Chiodini^{76a}, A.S. Chisholm³², A. Chitan^{28b}, Y.H. Chiu¹⁷², M.V. Chizhov⁶⁸, K. Choi⁶⁴, A.R. Chomont³⁷, S. Chouridou¹⁵⁶, Y.S. Chow^{62a}, V. Christodoulou⁸¹, M.C. Chu^{62a}, J. Chudoba¹²⁹, A.J. Chuinard⁹⁰, J.J. Chwastowski⁴², L. Chytka¹¹⁷, A.K. Ciftci^{4a}, D. Cinca⁴⁶, V. Cindro⁷⁸, I.A. Cioara²³, A. Ciochio¹⁶, F. Ciotto^{106a,106b}, Z.H. Citron¹⁷⁵, M. Citterio^{94a}, M. Ciubancan^{28b}, A. Clark⁵², B.L. Clark⁵⁹, M.R. Clark³⁸, P.J. Clark⁴⁹, R.N. Clarke¹⁶, C. Clement^{148a,148b}, Y. Coadou⁸⁸, M. Cobal^{167a,167c}, A. Coccaro⁵², J. Cochran⁶⁷, L. Colasurdo¹⁰⁸, B. Cole³⁸, A.P. Colijn¹⁰⁹, J. Collot⁵⁸, T. Colombo¹⁶⁶, P. Conde Muiño^{128a,128b}, E. Coniavitis⁵¹, S.H. Connell^{147b}, I.A. Connelly⁸⁷, S. Constantinescu^{28b}, G. Conti³², F. Conventi^{106a,n}, M. Cooke¹⁶, A.M. Cooper-Sarkar¹²², F. Cormier¹⁷¹, K.J.R. Cormier¹⁶¹, M. Corradi^{134a,134b}, F. Corriveau^{90,o}, A. Cortes-Gonzalez³², G. Costa^{94a}, M.J. Costa¹⁷⁰, D. Costanzo¹⁴¹, G. Cottin³⁰, G. Cowan⁸⁰, B.E. Cox⁸⁷, K. Cranmer¹¹², S.J. Crawley⁵⁶, R.A. Creager¹²⁴, G. Cree³¹, S. Crépé-Renaudin⁵⁸, F. Crescioli⁸³, W.A. Cribbs^{148a,148b}, M. Cristinziani²³, V. Croft¹¹², G. Crosetti^{40a,40b}, A. Cueto⁸⁵, T. Cuhadar Donszelmann¹⁴¹, A.R. Cukierman¹⁴⁵, J. Cummings¹⁷⁹, M. Curatolo⁵⁰, J. Cúth⁸⁶, S. Czekierda⁴², P. Czodrowski³², G. D'amen^{22a,22b}, S. D'Auria⁵⁶, L. D'eraimo⁸³, M. D'Onofrio⁷⁷, M.J. Da Cunha Sargedas De Sousa^{128a,128b}, C. Da Via⁸⁷, W. Dabrowski^{41a}, T. Dado^{146a}, T. Dai⁹², O. Dale¹⁵, F. Dallaire⁹⁷, C. Dallapiccola⁸⁹, M. Dam³⁹, J.R. Dandoy¹²⁴, M.F. Daneri²⁹, N.P. Dang¹⁷⁶, A.C. Daniells¹⁹, N.S. Dann⁸⁷, M. Danninger¹⁷¹, M. Dano Hoffmann¹³⁸, V. Dao¹⁵⁰, G. Darbo^{53a}, S. Darmora⁸, J. Dassoulas³, A. Dattagupta¹¹⁸, T. Daubney⁴⁵, W. Davey²³, C. David⁴⁵, T. Davidek¹³¹, D.R. Davis⁴⁸, P. Davison⁸¹, E. Dawe⁹¹, I. Dawson¹⁴¹, K. De⁸, R. de Asmundis^{106a}, A. De Benedetti¹¹⁵, S. De Castro^{22a,22b}, S. De Cecco⁸³, N. De Groot¹⁰⁸, P. de Jong¹⁰⁹, H. De la Torre⁹³, F. De Lorenzi⁶⁷, A. De Maria⁵⁷, D. De Pedis^{134a}, A. De Salvo^{134a}, U. De Sanctis^{135a,135b}, A. De Santo¹⁵¹, K. De Vasconcelos Corga⁸⁸, J.B. De Vivie De Regie¹¹⁹, R. Debbe²⁷, C. Debenedetti¹³⁹, D.V. Dedovich⁶⁸, N. Dehghanian³, I. Deigaard¹⁰⁹, M. Del Gaudio^{40a,40b}, J. Del Peso⁸⁵, D. Delgove¹¹⁹, F. Deliot¹³⁸, C.M. Delitzsch⁷, A. Dell'Acqua³², L. Dell'Asta²⁴, M. Dell'Orso^{126a,126b}, M. Della Pietra^{106a,106b}, D. della Volpe⁵², M. Delmastro⁵, C. Delporte¹¹⁹, P.A. Delsart⁵⁸, D.A. DeMarco¹⁶¹, S. Demers¹⁷⁹, M. Demichev⁶⁸, A. Demilly⁸³, S.P. Denisov¹³², D. Denysiuk¹³⁸, D. Derendarz⁴², J.E. Derkaoui^{137d}, F. Derue⁸³, P. Dervan⁷⁷, K. Desch²³, C. Deterre⁴⁵, K. Dette¹⁶¹, M.R. Devesa²⁹, P.O. Deviveiros³², A. Dewhurst¹³³, S. Dhaliwal²⁵, F.A. Di Bello⁵², A. Di Ciaccio^{135a,135b}, L. Di Ciaccio⁵, W.K. Di Clemente¹²⁴, C. Di Donato^{106a,106b}, A. Di Girolamo³², B. Di Girolamo³², B. Di Micco^{136a,136b}, R. Di Nardo³², K.F. Di Petrillo⁵⁹, A. Di Simone⁵¹, R. Di Sipio¹⁶¹, D. Di Valentino³¹, C. Diaconu⁸⁸, M. Diamond¹⁶¹, F.A. Dias³⁹, M.A. Diaz^{34a}, E.B. Diehl⁹², J. Dietrich¹⁷, S. Díez Cornell⁴⁵, A. Dimitrievska¹⁴, J. Dingfelder²³, P. Dita^{28b}, S. Dita^{28b}, F. Dittus³², F. Djama⁸⁸, T. Djobava^{54b}, J.I. Djuvsland^{60a}, M.A.B. do Vale^{26c}, D. Dobos³², M. Dobre^{28b}, D. Dodsworth²⁵, C. Doglioni⁸⁴,

J. Dolejsi ¹³¹, Z. Dolezal ¹³¹, M. Donadelli ^{26d}, S. Donati ^{126a,126b}, P. Dondero ^{123a,123b}, J. Donini ³⁷, J. Dopke ¹³³, A. Doria ^{106a}, M.T. Dova ⁷⁴, A.T. Doyle ⁵⁶, E. Drechsler ⁵⁷, M. Dris ¹⁰, Y. Du ^{36b}, J. Duarte-Camperderros ¹⁵⁵, A. Dubreuil ⁵², E. Duchovni ¹⁷⁵, G. Duckeck ¹⁰², A. Ducourthial ⁸³, O.A. Ducu ^{97,p}, D. Duda ¹⁰⁹, A. Dudarev ³², A. Chr. Dudder ⁸⁶, E.M. Duffield ¹⁶, L. Duflost ¹¹⁹, M. Dührssen ³², C. Dulsen ¹⁷⁸, M. Dumancic ¹⁷⁵, A.E. Dumitriu ^{28b}, A.K. Duncan ⁵⁶, M. Dunford ^{60a}, A. Duperrin ⁸⁸, H. Duran Yildiz ^{4a}, M. Düren ⁵⁵, A. Durglishvili ^{54b}, D. Duschinger ⁴⁷, B. Dutta ⁴⁵, D. Duvnjak ¹, M. Dyndal ⁴⁵, B.S. Dziedzic ⁴², C. Eckardt ⁴⁵, K.M. Ecker ¹⁰³, R.C. Edgar ⁹², T. Eifert ³², G. Eigen ¹⁵, K. Einsweiler ¹⁶, T. Ekelof ¹⁶⁸, M. El Kacimi ^{137c}, R. El Kosseifi ⁸⁸, V. Ellajosyula ⁸⁸, M. Ellert ¹⁶⁸, S. Elles ⁵, F. Ellinghaus ¹⁷⁸, A.A. Elliot ¹⁷², N. Ellis ³², J. Elmsheuser ²⁷, M. Elsing ³², D. Emelianov ¹³³, Y. Enari ¹⁵⁷, O.C. Endner ⁸⁶, J.S. Ennis ¹⁷³, M.B. Epland ⁴⁸, J. Erdmann ⁴⁶, A. Ereditato ¹⁸, M. Ernst ²⁷, S. Errede ¹⁶⁹, M. Escalier ¹¹⁹, C. Escobar ¹⁷⁰, B. Esposito ⁵⁰, O. Estrada Pastor ¹⁷⁰, A.I. Etienvre ¹³⁸, E. Etzion ¹⁵⁵, H. Evans ⁶⁴, A. Ezhilov ¹²⁵, M. Ezzi ^{137e}, F. Fabbri ^{22a,22b}, L. Fabbri ^{22a,22b}, V. Fabiani ¹⁰⁸, G. Facini ⁸¹, R.M. Fakhрутdinov ¹³², S. Falciano ^{134a}, R.J. Falla ⁸¹, J. Faltova ³², Y. Fang ^{35a}, M. Fanti ^{94a,94b}, A. Farbin ⁸, A. Farilla ^{136a}, C. Farina ¹²⁷, E.M. Farina ^{123a,123b}, T. Farooque ⁹³, S. Farrell ¹⁶, S.M. Farrington ¹⁷³, P. Farthouat ³², F. Fassi ^{137e}, P. Fassnacht ³², D. Fassouliotis ⁹, M. Faucci Giannelli ⁴⁹, A. Favareto ^{53a,53b}, W.J. Fawcett ¹²², L. Fayard ¹¹⁹, O.L. Fedin ^{125,q}, W. Fedorko ¹⁷¹, S. Feigl ¹²¹, L. Felgioni ⁸⁸, C. Feng ^{36b}, E.J. Feng ³², M.J. Fenton ⁵⁶, A.B. Fenyuk ¹³², L. Feremenga ⁸, P. Fernandez Martinez ¹⁷⁰, S. Fernandez Perez ¹³, J. Ferrando ⁴⁵, A. Ferrari ¹⁶⁸, P. Ferrari ¹⁰⁹, R. Ferrari ^{123a}, D.E. Ferreira de Lima ^{60b}, A. Ferrer ¹⁷⁰, D. Ferrere ⁵², C. Ferretti ⁹², F. Fiedler ⁸⁶, A. Filipčič ⁷⁸, M. Filipuzzi ⁴⁵, F. Filthaut ¹⁰⁸, M. Fincke-Keeler ¹⁷², K.D. Finelli ¹⁵², M.C.N. Fiolhais ^{128a,128c,r}, L. Fiorini ¹⁷⁰, A. Fischer ², C. Fischer ¹³, J. Fischer ¹⁷⁸, W.C. Fisher ⁹³, N. Flaschel ⁴⁵, I. Fleck ¹⁴³, P. Fleischmann ⁹², R.R.M. Fletcher ¹²⁴, T. Flick ¹⁷⁸, B.M. Flierl ¹⁰², L.R. Flores Castillo ^{62a}, M.J. Flowerdew ¹⁰³, G.T. Forcolin ⁸⁷, A. Formica ¹³⁸, F.A. Förster ¹³, A. Forti ⁸⁷, A.G. Foster ¹⁹, D. Fournier ¹¹⁹, H. Fox ⁷⁵, S. Fracchia ¹⁴¹, P. Francavilla ⁸³, M. Franchini ^{22a,22b}, S. Franchino ^{60a}, D. Francis ³², L. Franconi ¹²¹, M. Franklin ⁵⁹, M. Frate ¹⁶⁶, M. Fraternali ^{123a,123b}, D. Freeborn ⁸¹, S.M. Fressard-Batraneanu ³², B. Freund ⁹⁷, D. Froidevaux ³², J.A. Frost ¹²², C. Fukunaga ¹⁵⁸, T. Fusayasu ¹⁰⁴, J. Fuster ¹⁷⁰, O. Gabizon ¹⁵⁴, A. Gabrielli ^{22a,22b}, A. Gabrielli ¹⁶, G.P. Gach ^{41a}, S. Gadatsch ³², S. Gadomski ⁸⁰, G. Gagliardi ^{53a,53b}, L.G. Gagnon ⁹⁷, C. Galea ¹⁰⁸, B. Galhardo ^{128a,128c}, E.J. Gallas ¹²², B.J. Gallop ¹³³, P. Gallus ¹³⁰, G. Galster ³⁹, K.K. Gan ¹¹³, S. Ganguly ³⁷, Y. Gao ⁷⁷, Y.S. Gao ^{145,g}, F.M. Garay Walls ^{34a}, C. García ¹⁷⁰, J.E. García Navarro ¹⁷⁰, J.A. García Pascual ^{35a}, M. Garcia-Sciveres ¹⁶, R.W. Gardner ³³, N. Garelli ¹⁴⁵, V. Garonne ¹²¹, A. Gascon Bravo ⁴⁵, K. Gasnikova ⁴⁵, C. Gatti ⁵⁰, A. Gaudiello ^{53a,53b}, G. Gaudio ^{123a}, I.L. Gavrilenko ⁹⁸, C. Gay ¹⁷¹, G. Gaycken ²³, E.N. Gazis ¹⁰, C.N.P. Gee ¹³³, J. Geisen ⁵⁷, M. Geisen ⁸⁶, M.P. Geisler ^{60a}, K. Gellerstedt ^{148a,148b}, C. Gemme ^{53a}, M.H. Genest ⁵⁸, C. Geng ⁹², S. Gentile ^{134a,134b}, C. Gentsos ¹⁵⁶, S. George ⁸⁰, D. Gerbaudo ¹³, G. Geßner ⁴⁶, S. Ghasemi ¹⁴³, M. Ghneimat ²³, B. Giacobbe ^{22a}, S. Giagu ^{134a,134b}, N. Giangiacomi ^{22a,22b}, P. Giannetti ^{126a,126b}, S.M. Gibson ⁸⁰, M. Gignac ¹⁷¹, M. Gilchriese ¹⁶, D. Gillberg ³¹, G. Gilles ¹⁷⁸, D.M. Gingrich ^{3,d}, M.P. Giordani ^{167a,167c}, F.M. Giorgi ^{22a}, P.F. Giraud ¹³⁸, P. Giromini ⁵⁹, G. Giugliarelli ^{167a,167c}, D. Giugni ^{94a}, F. Giuli ¹²², C. Giuliani ¹⁰³, M. Giulini ^{60b}, B.K. Gjeltzen ¹²¹, S. Gkaitatzis ¹⁵⁶, I. Gkialas ^{9,s}, E.L. Gkoukousis ¹³, P. Gkoutoumis ¹⁰, L.K. Gladilin ¹⁰¹, C. Glasman ⁸⁵, J. Glatzer ¹³, P.C.F. Glaysher ⁴⁵, A. Glazov ⁴⁵, M. Goblirsch-Kolb ²⁵, J. Godlewski ⁴², S. Goldfarb ⁹¹, T. Golling ⁵², D. Golubkov ¹³², A. Gomes ^{128a,128b,128d}, R. Gonçalves ^{128a}, R. Goncalves Gama ^{26a}, J. Goncalves Pinto Firmino Da Costa ¹³⁸, G. Gonella ⁵¹, L. Gonella ¹⁹, A. Gongadze ⁶⁸, S. González de la Hoz ¹⁷⁰, S. Gonzalez-Sevilla ⁵², L. Goossens ³², P.A. Gorbounov ⁹⁹, H.A. Gordon ²⁷, I. Gorelov ¹⁰⁷, B. Gorini ³², E. Gorini ^{76a,76b}, A. Gorišek ⁷⁸, A.T. Goshaw ⁴⁸, C. Gössling ⁴⁶, M.I. Gostkin ⁶⁸, C.A. Gottardo ²³, C.R. Goudet ¹¹⁹, D. Goujdami ^{137c}, A.G. Goussiou ¹⁴⁰, N. Govender ^{147b,t}, E. Gozani ¹⁵⁴, I. Grabowska-Bold ^{41a}, P.O.J. Gradin ¹⁶⁸, J. Gramling ¹⁶⁶, E. Gramstad ¹²¹, S. Grancagnolo ¹⁷, V. Gratchev ¹²⁵, P.M. Gravila ^{28f}, C. Gray ⁵⁶, H.M. Gray ¹⁶, Z.D. Greenwood ^{82,u}, C. Grefe ²³, K. Gregersen ⁸¹, I.M. Gregor ⁴⁵, P. Grenier ¹⁴⁵, K. Grevtsov ⁵, J. Griffiths ⁸, A.A. Grillo ¹³⁹, K. Grimm ⁷⁵, S. Grinstein ^{13,v}, Ph. Gris ³⁷, J.-F. Grivaz ¹¹⁹, S. Groh ⁸⁶, E. Gross ¹⁷⁵, J. Grosse-Knetter ⁵⁷, G.C. Grossi ⁸², Z.J. Grout ⁸¹, A. Grummer ¹⁰⁷, L. Guan ⁹², W. Guan ¹⁷⁶, J. Guenther ³², F. Guescini ^{163a}, D. Guest ¹⁶⁶, O. Gueta ¹⁵⁵, B. Gui ¹¹³, E. Guido ^{53a,53b}, T. Guillemin ⁵, S. Guindon ³², U. Gul ⁵⁶, C. Gumpert ³², J. Guo ^{36c}, W. Guo ⁹², Y. Guo ^{36a,w}, R. Gupta ⁴³, S. Gupta ¹²², S. Gurbuz ^{20a}, G. Gustavino ¹¹⁵, B.J. Gutelman ¹⁵⁴, P. Gutierrez ¹¹⁵, N.G. Gutierrez Ortiz ⁸¹, C. Gutsche ⁸¹, C. Guyot ¹³⁸, M.P. Guzik ^{41a}, C. Gwenlan ¹²², C.B. Gwilliam ⁷⁷,

A. Haas¹¹², C. Haber¹⁶, H.K. Hadavand⁸, N. Haddad^{137e}, A. Hadeef⁸⁸, S. Hageböck²³, M. Hagihara¹⁶⁴, H. Hakobyan^{180,*}, M. Haleem⁴⁵, J. Haley¹¹⁶, G. Halladjian⁹³, G.D. Hallewell⁸⁸, K. Hamacher¹⁷⁸, P. Hamal¹¹⁷, K. Hamano¹⁷², A. Hamilton^{147a}, G.N. Hamity¹⁴¹, P.G. Hamnett⁴⁵, L. Han^{36a}, S. Han^{35a}, K. Hanagaki^{69,x}, K. Hanawa¹⁵⁷, M. Hance¹³⁹, B. Haney¹²⁴, P. Hanke^{60a}, J.B. Hansen³⁹, J.D. Hansen³⁹, M.C. Hansen²³, P.H. Hansen³⁹, K. Hara¹⁶⁴, A.S. Hard¹⁷⁶, T. Harenberg¹⁷⁸, F. Hariri¹¹⁹, S. Harkusha⁹⁵, P.F. Harrison¹⁷³, N.M. Hartmann¹⁰², Y. Hasegawa¹⁴², A. Hasib⁴⁹, S. Hassani¹³⁸, S. Haug¹⁸, R. Hauser⁹³, L. Hauswald⁴⁷, L.B. Havener³⁸, M. Havranek¹³⁰, C.M. Hawkes¹⁹, R.J. Hawking³², D. Hayakawa¹⁵⁹, D. Hayden⁹³, C.P. Hays¹²², J.M. Hays⁷⁹, H.S. Hayward⁷⁷, S.J. Haywood¹³³, S.J. Head¹⁹, T. Heck⁸⁶, V. Hedberg⁸⁴, L. Heelan⁸, S. Heer²³, K.K. Heidegger⁵¹, S. Heim⁴⁵, T. Heim¹⁶, B. Heinemann^{45,y}, J.J. Heinrich¹⁰², L. Heinrich¹¹², C. Heinz⁵⁵, J. Hejbal¹²⁹, L. Helary³², A. Held¹⁷¹, S. Hellman^{148a,148b}, C. Helsen³², R.C.W. Henderson⁷⁵, Y. Heng¹⁷⁶, S. Henkelmann¹⁷¹, A.M. Henriques Correia³², S. Henrot-Versille¹¹⁹, G.H. Herbert¹⁷, H. Herde²⁵, V. Herget¹⁷⁷, Y. Hernández Jiménez^{147c}, H. Herr⁸⁶, G. Herten⁵¹, R. Hertenberger¹⁰², L. Hervas³², T.C. Herwig¹²⁴, G.G. Hesketh⁸¹, N.P. Hessey^{163a}, J.W. Hetherly⁴³, S. Higashino⁶⁹, E. Higón-Rodríguez¹⁷⁰, K. Hildebrand³³, E. Hill¹⁷², J.C. Hill³⁰, K.H. Hiller⁴⁵, S.J. Hillier¹⁹, M. Hils⁴⁷, I. Hinchliffe¹⁶, M. Hirose⁵¹, D. Hirschbuehl¹⁷⁸, B. Hiti⁷⁸, O. Hladik¹²⁹, X. Hoad⁴⁹, J. Hobbs¹⁵⁰, N. Hod^{163a}, M.C. Hodgkinson¹⁴¹, P. Hodgson¹⁴¹, A. Hoecker³², M.R. Hoferkamp¹⁰⁷, F. Hoenig¹⁰², D. Hohn²³, T.R. Holmes³³, M. Homann⁴⁶, S. Honda¹⁶⁴, T. Honda⁶⁹, T.M. Hong¹²⁷, B.H. Hooberman¹⁶⁹, W.H. Hopkins¹¹⁸, Y. Horii¹⁰⁵, A.J. Horton¹⁴⁴, J-Y. Hostachy⁵⁸, A. Hostiuc¹⁴⁰, S. Hou¹⁵³, A. Hoummada^{137a}, J. Howarth⁸⁷, J. Hoya⁷⁴, M. Hrabovsky¹¹⁷, J. Hrdinka³², I. Hristova¹⁷, J. Hrivnac¹¹⁹, T. Hryn'ova⁵, A. Hrynevich⁹⁶, P.J. Hsu⁶³, S.-C. Hsu¹⁴⁰, Q. Hu^{36a}, S. Hu^{36c}, Y. Huang^{35a}, Z. Hubacek¹³⁰, F. Hubaut⁸⁸, F. Huegging²³, T.B. Huffman¹²², E.W. Hughes³⁸, G. Hughes⁷⁵, M. Huhtinen³², R.F.H. Hunter³¹, P. Huo¹⁵⁰, N. Huseynov^{68,b}, J. Huston⁹³, J. Huth⁵⁹, R. Hyneman⁹², G. Iacobucci⁵², G. Iakovidis²⁷, I. Ibragimov¹⁴³, L. Iconomidou-Fayard¹¹⁹, Z. Idrissi^{137e}, P. Iengo³², O. Igonkina^{109,z}, T. Iizawa¹⁷⁴, Y. Ikegami⁶⁹, M. Ikeno⁶⁹, Y. Ilchenko^{11,aa}, D. Iliadis¹⁵⁶, N. Ilic¹⁴⁵, F. Iltzsche⁴⁷, G. Introzzi^{123a,123b}, P. Ioannou^{9,*}, M. Iodice^{136a}, K. Iordanidou³⁸, V. Ippolito⁵⁹, M.F. Isacson¹⁶⁸, N. Ishijima¹²⁰, M. Ishino¹⁵⁷, M. Ishitsuka¹⁵⁹, C. Issever¹²², S. Istin^{20a}, F. Ito¹⁶⁴, J.M. Iturbe Ponce^{62a}, R. Iuppa^{162a,162b}, H. Iwasaki⁶⁹, J.M. Izen⁴⁴, V. Izzo^{106a}, S. Jabbar³, P. Jackson¹, R.M. Jacobs²³, V. Jain², K.B. Jakobi⁸⁶, K. Jakobs⁵¹, S. Jakobsen⁶⁵, T. Jakoubek¹²⁹, D.O. Jamin¹¹⁶, D.K. Jana⁸², R. Jansky⁵², J. Janssen²³, M. Janus⁵⁷, P.A. Janus^{41a}, G. Jarlskog⁸⁴, N. Javadov^{68,b}, T. Javůrek⁵¹, M. Javurkova⁵¹, F. Jeanneau¹³⁸, L. Jeanty¹⁶, J. Jejelava^{54a,ab}, A. Jelinskas¹⁷³, P. Jenni^{51,ac}, C. Jeske¹⁷³, S. Jézéquel⁵, H. Ji¹⁷⁶, J. Jia¹⁵⁰, H. Jiang⁶⁷, Y. Jiang^{36a}, Z. Jiang¹⁴⁵, S. Jiggins⁸¹, J. Jimenez Pena¹⁷⁰, S. Jin^{35a}, A. Jinaru^{28b}, O. Jinnouchi¹⁵⁹, H. Jivan^{147c}, P. Johansson¹⁴¹, K.A. Johns⁷, C.A. Johnson⁶⁴, W.J. Johnson¹⁴⁰, K. Jon-And^{148a,148b}, R.W.L. Jones⁷⁵, S.D. Jones¹⁵¹, S. Jones⁷, T.J. Jones⁷⁷, J. Jongmanns^{60a}, P.M. Jorge^{128a,128b}, J. Jovicevic^{163a}, X. Ju¹⁷⁶, A. Juste Rozas^{13,v}, M.K. Köhler¹⁷⁵, A. Kaczmarska⁴², M. Kado¹¹⁹, H. Kagan¹¹³, M. Kagan¹⁴⁵, S.J. Kahn⁸⁸, T. Kaji¹⁷⁴, E. Kajomovitz¹⁵⁴, C.W. Kalderon⁸⁴, A. Kaluza⁸⁶, S. Kama⁴³, A. Kamenshchikov¹³², N. Kanaya¹⁵⁷, L. Kanjir⁷⁸, V.A. Kantserov¹⁰⁰, J. Kanzaki⁶⁹, B. Kaplan¹¹², L.S. Kaplan¹⁷⁶, D. Kar^{147c}, K. Karakostas¹⁰, N. Karastathis¹⁰, M.J. Kareem^{163b}, E. Karentzos¹⁰, S.N. Karpov⁶⁸, Z.M. Karpova⁶⁸, K. Karthik¹¹², V. Kartvelishvili⁷⁵, A.N. Karyukhin¹³², K. Kasahara¹⁶⁴, L. Kashif¹⁷⁶, R.D. Kass¹¹³, A. Kastanas¹⁴⁹, Y. Kataoka¹⁵⁷, C. Kato¹⁵⁷, A. Katre⁵², J. Katzy⁴⁵, K. Kawade⁷⁰, K. Kawagoe⁷³, T. Kawamoto¹⁵⁷, G. Kawamura⁵⁷, E.F. Kay⁷⁷, V.F. Kazanin^{111,c}, R. Keeler¹⁷², R. Kehoe⁴³, J.S. Keller³¹, E. Kellermann⁸⁴, J.J. Kempster⁸⁰, J. Kendrick¹⁹, H. Keoshkerian¹⁶¹, O. Kepka¹²⁹, B.P. Kerševan⁷⁸, S. Kersten¹⁷⁸, R.A. Keyes⁹⁰, M. Khader¹⁶⁹, F. Khalil-zada¹², A. Khanov¹¹⁶, A.G. Kharlamov^{111,c}, T. Kharlamova^{111,c}, A. Khodinov¹⁶⁰, T.J. Khoo⁵², V. Khovanskiy^{99,*}, E. Khramov⁶⁸, J. Khubua^{54b,ad}, S. Kido⁷⁰, C.R. Kilby⁸⁰, H.Y. Kim⁸, S.H. Kim¹⁶⁴, Y.K. Kim³³, N. Kimura¹⁵⁶, O.M. Kind¹⁷, B.T. King⁷⁷, D. Kirchmeier⁴⁷, J. Kirk¹³³, A.E. Kiryunin¹⁰³, T. Kishimoto¹⁵⁷, D. Kisielewska^{41a}, V. Kitali⁴⁵, O. Kivernyk⁵, E. Kladiva^{146b}, T. Klapdor-Kleingrothaus⁵¹, M.H. Klein⁹², M. Klein⁷⁷, U. Klein⁷⁷, K. Kleinknecht⁸⁶, P. Klimek¹¹⁰, A. Klimentov²⁷, R. Klingenberg⁴⁶, T. Klingl²³, T. Klioutchnikova³², E.-E. Kluge^{60a}, P. Kluit¹⁰⁹, S. Kluth¹⁰³, E. Kneringer⁶⁵, E.B.F.G. Knoop⁸⁸, A. Knue¹⁰³, A. Kobayashi¹⁵⁷, D. Kobayashi⁷³, T. Kobayashi¹⁵⁷, M. Kobel⁴⁷, M. Kocian¹⁴⁵, P. Kodys¹³¹, T. Koffas³¹, E. Koffeman¹⁰⁹, N.M. Köhler¹⁰³, T. Koi¹⁴⁵, M. Kolb^{60b}, I. Koletsou⁵, A.A. Komar^{98,*}, T. Kondo⁶⁹, N. Kondrashova^{36c}, K. Köneke⁵¹, A.C. König¹⁰⁸, T. Kono^{69,ae}, R. Konoplich^{112,af}, N. Konstantinidis⁸¹, R. Kopeliansky⁶⁴, S. Kopperny^{41a},

A.K. Kopp⁵¹, K. Korcyl⁴², K. Kordas¹⁵⁶, A. Korn⁸¹, A.A. Korol^{111,c}, I. Korolkov¹³, E.V. Korolkova¹⁴¹, O. Kortner¹⁰³, S. Kortner¹⁰³, T. Kosek¹³¹, V.V. Kostyukhin²³, A. Kotwal⁴⁸, A. Koulouris¹⁰, A. Kourkouveli-Charalampidi^{123a,123b}, C. Kourkouvelis⁹, E. Kourlitis¹⁴¹, V. Kouskoura²⁷, A.B. Kowalewska⁴², R. Kowalewski¹⁷², T.Z. Kowalski^{41a}, C. Kozakai¹⁵⁷, W. Kozanecki¹³⁸, A.S. Kozhin¹³², V.A. Kramarenko¹⁰¹, G. Kramberger⁷⁸, D. Krasnopevtsev¹⁰⁰, M.W. Krasny⁸³, A. Krasznahorkay³², D. Krauss¹⁰³, J.A. Kremer^{41a}, J. Kretzschmar⁷⁷, K. Kreutzfeldt⁵⁵, P. Krieger¹⁶¹, K. Krizka¹⁶, K. Kroeninger⁴⁶, H. Kroha¹⁰³, J. Kroll¹²⁹, J. Kroll¹²⁴, J. Kroseberg²³, J. Krstic¹⁴, U. Kruchonak⁶⁸, H. Krüger²³, N. Krumnack⁶⁷, M.C. Kruse⁴⁸, T. Kubota⁹¹, H. Kucuk⁸¹, S. Kuday^{4b}, J.T. Kuechler¹⁷⁸, S. Kuehn³², A. Kugel^{60a}, F. Kuger¹⁷⁷, T. Kuhl⁴⁵, V. Kukhtin⁶⁸, R. Kukla⁸⁸, Y. Kulchitsky⁹⁵, S. Kuleshov^{34b}, Y.P. Kulinich¹⁶⁹, M. Kuna^{134a,134b}, T. Kunigo⁷¹, A. Kupco¹²⁹, T. Kupfer⁴⁶, O. Kuprash¹⁵⁵, H. Kurashige⁷⁰, L.L. Kurchaninov^{163a}, Y.A. Kurochkin⁹⁵, M.G. Kurth^{35a}, E.S. Kuwertz¹⁷², M. Kuze¹⁵⁹, J. Kvita¹¹⁷, T. Kwan¹⁷², D. Kyriazopoulos¹⁴¹, A. La Rosa¹⁰³, J.L. La Rosa Navarro^{26d}, L. La Rotonda^{40a,40b}, F. La Ruffa^{40a,40b}, C. Lacasta¹⁷⁰, F. Lacava^{134a,134b}, J. Lacey⁴⁵, D.P.J. Lack⁸⁷, H. Lacker¹⁷, D. Lacour⁸³, E. Ladygin⁶⁸, R. Lafaye⁵, B. Laforge⁸³, T. Lagouri¹⁷⁹, S. Lai⁵⁷, S. Lammers⁶⁴, W. Lampl⁷, E. Lançon²⁷, U. Landgraf⁵¹, M.P.J. Landon⁷⁹, M.C. Lanfermann⁵², V.S. Lang⁴⁵, J.C. Lange¹³, R.J. Langenberg³², A.J. Lankford¹⁶⁶, F. Lanni²⁷, K. Lantzsch²³, A. Lanza^{123a}, A. Lapertosa^{53a,53b}, S. Laplace⁸³, J.F. Laporte¹³⁸, T. Lari^{94a}, F. Lasagni Manghi^{22a,22b}, M. Lassnig³², T.S. Lau^{62a}, P. Laurelli⁵⁰, W. Lavrijsen¹⁶, A.T. Law¹³⁹, P. Laycock⁷⁷, T. Lazovich⁵⁹, M. Lazzaroni^{94a,94b}, B. Le⁹¹, O. Le Dortz⁸³, E. Le Guirriec⁸⁸, E.P. Le Quilleuc¹³⁸, M. LeBlanc¹⁷², T. LeCompte⁶, F. Ledroit-Guillon⁵⁸, C.A. Lee²⁷, G.R. Lee^{34a}, S.C. Lee¹⁵³, L. Lee⁵⁹, B. Lefebvre⁹⁰, G. Lefebvre⁸³, M. Lefebvre¹⁷², F. Legger¹⁰², C. Leggett¹⁶, G. Lehmann Miotto³², X. Lei⁷, W.A. Leight⁴⁵, M.A.L. Leite^{26d}, R. Leitner¹³¹, D. Lellouch¹⁷⁵, B. Lemmer⁵⁷, K.J.C. Leney⁸¹, T. Lenz²³, B. Lenzi³², R. Leone⁷, S. Leone^{126a,126b}, C. Leonidopoulos⁴⁹, G. Lerner¹⁵¹, C. Leroy⁹⁷, R. Les¹⁶¹, A.A.J. Lesage¹³⁸, C.G. Lester³⁰, M. Levchenko¹²⁵, J. Levêque⁵, D. Levin⁹², L.J. Levinson¹⁷⁵, M. Levy¹⁹, D. Lewis⁷⁹, B. Li^{36a,w}, Changqiao Li^{36a}, H. Li¹⁵⁰, L. Li^{36c}, Q. Li^{35a}, Q. Li^{36a}, S. Li⁴⁸, X. Li^{36c}, Y. Li¹⁴³, Z. Liang^{35a}, B. Liberti^{135a}, A. Liblong¹⁶¹, K. Lie^{62c}, J. Liebal²³, W. Liebig¹⁵, A. Limosani¹⁵², K. Lin⁹³, S.C. Lin¹⁸², T.H. Lin⁸⁶, R.A. Linck⁶⁴, B.E. Lindquist¹⁵⁰, A.E. Lioni⁵², E. Lipeles¹²⁴, A. Lipniacka¹⁵, M. Lisovsky^{60b}, T.M. Liss^{169,ag}, A. Lister¹⁷¹, A.M. Litke¹³⁹, B. Liu⁶⁷, H. Liu⁹², H. Liu²⁷, J.K.K. Liu¹²², J. Liu^{36b}, J.B. Liu^{36a}, K. Liu⁸⁸, L. Liu¹⁶⁹, M. Liu^{36a}, Y.L. Liu^{36a}, Y. Liu^{36a}, M. Livan^{123a,123b}, A. Lleres⁵⁸, J. Llorente Merino^{35a}, S.L. Lloyd⁷⁹, C.Y. Lo^{62b}, F. Lo Sterzo⁴³, E.M. Lobodzinska⁴⁵, P. Loch⁷, F.K. Loebinger⁸⁷, A. Loesle⁵¹, K.M. Loew²⁵, T. Lohse¹⁷, K. Lohwasser¹⁴¹, M. Lokajicek¹²⁹, B.A. Long²⁴, J.D. Long¹⁶⁹, R.E. Long⁷⁵, L. Longo^{76a,76b}, K.A. Looper¹¹³, J.A. Lopez^{34b}, I. Lopez Paz¹³, A. Lopez Solis⁸³, J. Lorenz¹⁰², N. Lorenzo Martinez⁵, M. Losada²¹, P.J. Lösel¹⁰², X. Lou^{35a}, A. Lounis¹¹⁹, J. Love⁶, P.A. Love⁷⁵, H. Lu^{62a}, N. Lu⁹², Y.J. Lu⁶³, H.J. Lubatti¹⁴⁰, C. Luci^{134a,134b}, A. Lucotte⁵⁸, C. Luedtke⁵¹, F. Luehring⁶⁴, W. Lukas⁶⁵, L. Luminari^{134a}, O. Lundberg^{148a,148b}, B. Lund-Jensen¹⁴⁹, M.S. Lutz⁸⁹, P.M. Luzi⁸³, D. Lynn²⁷, R. Lysak¹²⁹, E. Lytken⁸⁴, F. Lyu^{35a}, V. Lyubushkin⁶⁸, H. Ma²⁷, L.L. Ma^{36b}, Y. Ma^{36b}, G. Maccarrone⁵⁰, A. Macchiolo¹⁰³, C.M. Macdonald¹⁴¹, B. Maček⁷⁸, J. Machado Miguens^{124,128b}, D. Madaffari¹⁷⁰, R. Madar³⁷, W.F. Mader⁴⁷, A. Madsen⁴⁵, N. Madysa⁴⁷, J. Maeda⁷⁰, S. Maeland¹⁵, T. Maeno²⁷, A.S. Maevskiy¹⁰¹, V. Magerl⁵¹, C. Maiani¹¹⁹, C. Maidantchik^{26a}, T. Maier¹⁰², A. Maio^{128a,128b,128d}, O. Majersky^{146a}, S. Majewski¹¹⁸, Y. Makida⁶⁹, N. Makovec¹¹⁹, B. Malaescu⁸³, Pa. Malecki⁴², V.P. Maleev¹²⁵, F. Malek⁵⁸, U. Mallik⁶⁶, D. Malon⁶, C. Malone³⁰, S. Maltezos¹⁰, S. Malyukov³², J. Mamuzic¹⁷⁰, G. Mancini⁵⁰, I. Mandić⁷⁸, J. Maneira^{128a,128b}, L. Manhaes de Andrade Filho^{26b}, J. Manjarres Ramos⁴⁷, K.H. Mankinen⁸⁴, A. Mann¹⁰², A. Manousos³², B. Mansoulie¹³⁸, J.D. Mansour^{35a}, R. Mantifel⁹⁰, M. Mantoani⁵⁷, S. Manzoni^{94a,94b}, L. Mapelli³², G. Marceca²⁹, L. March⁵², L. Marchese¹²², G. Marchiori⁸³, M. Marcisovsky¹²⁹, C.A. Marin Tobon³², M. Marjanovic³⁷, D.E. Marley⁹², F. Marroquim^{26a}, S.P. Marsden⁸⁷, Z. Marshall¹⁶, M.U.F. Martensson¹⁶⁸, S. Marti-Garcia¹⁷⁰, C.B. Martin¹¹³, T.A. Martin¹⁷³, V.J. Martin⁴⁹, B. Martin dit Latour¹⁵, M. Martinez^{13,v}, V.I. Martinez Outschoorn¹⁶⁹, S. Martin-Haugh¹³³, V.S. Martoiu^{28b}, A.C. Martyniuk⁸¹, A. Marzin³², L. Masetti⁸⁶, T. Mashimo¹⁵⁷, R. Mashinistov⁹⁸, J. Masik⁸⁷, A.L. Maslennikov^{111,c}, L.H. Mason⁹¹, L. Massa^{135a,135b}, P. Mastrandrea⁵, A. Mastroberardino^{40a,40b}, T. Masubuchi¹⁵⁷, P. Mättig¹⁷⁸, J. Maurer^{28b}, S.J. Maxfield⁷⁷, D.A. Maximov^{111,c}, R. Mazini¹⁵³, I. Maznas¹⁵⁶, S.M. Mazza^{94a,94b}, N.C. Mc Fadden¹⁰⁷, G. Mc Goldrick¹⁶¹, S.P. Mc Kee⁹², A. McCarn⁹², R.L. McCarthy¹⁵⁰, T.G. McCarthy¹⁰³, L.I. McClymont⁸¹,

E.F. McDonald⁹¹, J.A. Mcfayden³², G. Mchedlidze⁵⁷, S.J. McMahon¹³³, P.C. McNamara⁹¹, C.J. McNicol¹⁷³, R.A. McPherson^{172,o}, Z.A. Meadows⁸⁹, S. Meehan¹⁴⁰, T.J. Megy⁵¹, S. Mehlhase¹⁰², A. Mehta⁷⁷, T. Meideck⁵⁸, K. Meier^{60a}, B. Meirose⁴⁴, D. Melini^{170,ah}, B.R. Mellado Garcia^{147c}, J.D. Mellenthin⁵⁷, M. Melo^{146a}, F. Meloni¹⁸, A. Melzer²³, S.B. Menary⁸⁷, L. Meng⁷⁷, X.T. Meng⁹², A. Mengarelli^{22a,22b}, S. Menke¹⁰³, E. Meoni^{40a,40b}, S. Mergelmeyer¹⁷, C. Merlassino¹⁸, P. Mermod⁵², L. Merola^{106a,106b}, C. Meroni^{94a}, F.S. Merritt³³, A. Messina^{134a,134b}, J. Metcalfe⁶, A.S. Mete¹⁶⁶, C. Meyer¹²⁴, J.-P. Meyer¹³⁸, J. Meyer¹⁰⁹, H. Meyer Zu Theenhausen^{60a}, F. Miano¹⁵¹, R.P. Middleton¹³³, S. Miglioranza^{53a,53b}, L. Mijović⁴⁹, G. Mikenberg¹⁷⁵, M. Mikestikova¹²⁹, M. Mikuz⁷⁸, M. Milesi⁹¹, A. Milic¹⁶¹, D.A. Millar⁷⁹, D.W. Miller³³, C. Mills⁴⁹, A. Milov¹⁷⁵, D.A. Milstead^{148a,148b}, A.A. Minaenko¹³², Y. Minami¹⁵⁷, I.A. Minashvili^{54b}, A.I. Mincer¹¹², B. Mindur^{41a}, M. Mineev⁶⁸, Y. Minegishi¹⁵⁷, Y. Ming¹⁷⁶, L.M. Mir¹³, A. Mirto^{76a,76b}, K.P. Mistry¹²⁴, T. Mitani¹⁷⁴, J. Mitrevski¹⁰², V.A. Mitsou¹⁷⁰, A. Miucci¹⁸, P.S. Miyagawa¹⁴¹, A. Mizukami⁶⁹, J.U. Mjörnmark⁸⁴, T. Mkrtchyan¹⁸⁰, M. Mlynarikova¹³¹, T. Moa^{148a,148b}, K. Mochizuki⁹⁷, P. Mogg⁵¹, S. Mohapatra³⁸, S. Molander^{148a,148b}, R. Moles-Valls²³, M.C. Mondragon⁹³, K. Mönig⁴⁵, J. Monk³⁹, E. Monnier⁸⁸, A. Montalbano¹⁵⁰, J. Montejo Berlingen³², F. Monticelli⁷⁴, S. Monzani^{94a,94b}, R.W. Moore³, N. Morange¹¹⁹, D. Moreno²¹, M. Moreno Llácer³², P. Morettini^{53a}, S. Morgenstern³², D. Mori¹⁴⁴, T. Mori¹⁵⁷, M. Morii⁵⁹, M. Morinaga¹⁷⁴, V. Morisbak¹²¹, A.K. Morley³², G. Mornacchi³², J.D. Morris⁷⁹, L. Morvaj¹⁵⁰, P. Moschovakos¹⁰, M. Mosidze^{54b}, H.J. Moss¹⁴¹, J. Moss^{145,ai}, K. Motohashi¹⁵⁹, R. Mount¹⁴⁵, E. Mountricha²⁷, E.J.W. Moyse⁸⁹, S. Muanza⁸⁸, F. Mueller¹⁰³, J. Mueller¹²⁷, R.S.P. Mueller¹⁰², D. Muenstermann⁷⁵, P. Mullen⁵⁶, G.A. Mullier¹⁸, F.J. Munoz Sanchez⁸⁷, W.J. Murray^{173,133}, H. Musheghyan³², M. Muškinja⁷⁸, A.G. Myagkov^{132,qj}, M. Myska¹³⁰, B.P. Nachman¹⁶, O. Nackenhorst⁵², K. Nagai¹²², R. Nagai^{69,ae}, K. Nagano⁶⁹, Y. Nagasaka⁶¹, K. Nagata¹⁶⁴, M. Nagel⁵¹, E. Nagy⁸⁸, A.M. Nairz³², Y. Nakahama¹⁰⁵, K. Nakamura⁶⁹, T. Nakamura¹⁵⁷, I. Nakano¹¹⁴, R.F. Naranjo Garcia⁴⁵, R. Narayan¹¹, D.I. Narrias Villar^{60a}, I. Naryshkin¹²⁵, T. Naumann⁴⁵, G. Navarro²¹, R. Nayyar⁷, H.A. Neal⁹², P.Yu. Nechaeva⁹⁸, T.J. Neep¹³⁸, A. Negri^{123a,123b}, M. Negrini^{22a}, S. Nektarijevic¹⁰⁸, C. Nellist⁵⁷, A. Nelson¹⁶⁶, M.E. Nelson¹²², S. Nemecek¹²⁹, P. Nemethy¹¹², M. Nessi^{32,ak}, M.S. Neubauer¹⁶⁹, M. Neumann¹⁷⁸, P.R. Newman¹⁹, T.Y. Ng^{62c}, T. Nguyen Manh⁹⁷, R.B. Nickerson¹²², R. Nicolaidou¹³⁸, J. Nielsen¹³⁹, N. Nikiforou¹¹, V. Nikolaenko^{132,qj}, I. Nikolic-Audit⁸³, K. Nikolopoulos¹⁹, J.K. Nilsen¹²¹, P. Nilsson²⁷, Y. Ninomiya¹⁵⁷, A. Nisati^{134a}, N. Nishu^{36c}, R. Nisius¹⁰³, I. Nitsche⁴⁶, T. Nitta¹⁷⁴, T. Nobe¹⁵⁷, Y. Noguchi⁷¹, M. Nomachi¹²⁰, I. Nomidis³¹, M.A. Nomura²⁷, T. Nooney⁷⁹, M. Nordberg³², N. Norjoharuddeen¹²², O. Novgorodova⁴⁷, M. Nozaki⁶⁹, L. Nozka¹¹⁷, K. Ntekas¹⁶⁶, E. Nurse⁸¹, F. Nuti⁹¹, K. O'Connor²⁵, D.C. O'Neil¹⁴⁴, A.A. O'Rourke⁴⁵, V. O'Shea⁵⁶, F.G. Oakham^{31,d}, H. Oberlack¹⁰³, T. Obermann²³, J. Ocariz⁸³, A. Ochi⁷⁰, I. Ochoa³⁸, J.P. Ochoa-Ricoux^{34a}, S. Oda⁷³, S. Odaka⁶⁹, A. Oh⁸⁷, S.H. Oh⁴⁸, C.C. Ohm¹⁴⁹, H. Ohman¹⁶⁸, H. Oide^{53a,53b}, H. Okawa¹⁶⁴, Y. Okumura¹⁵⁷, T. Okuyama⁶⁹, A. Olariu^{28b}, L.F. Oleiro Seabra^{128a}, S.A. Olivares Pino^{34a}, D. Oliveira Damazio²⁷, A. Olszewski⁴², J. Olszowska⁴², A. Onofre^{128a,128e}, K. Onogi¹⁰⁵, P.U.E. Onyisi^{11,aa}, H. Oppen¹²¹, M.J. Oreglia³³, Y. Oren¹⁵⁵, D. Orestano^{136a,136b}, N. Orlando^{62b}, R.S. Orr¹⁶¹, B. Osculati^{53a,53b,*}, R. Ospanov^{36a}, G. Otero y Garzon²⁹, H. Otono⁷³, M. Ouchrif^{137d}, F. Ould-Saada¹²¹, A. Ouraou¹³⁸, K.P. Oussoren¹⁰⁹, Q. Ouyang^{35a}, M. Owen⁵⁶, R.E. Owen¹⁹, V.E. Ozcan^{20a}, N. Ozturk⁸, K. Pachal¹⁴⁴, A. Pacheco Pages¹³, L. Pacheco Rodriguez¹³⁸, C. Padilla Aranda¹³, S. Pagan Griso¹⁶, M. Paganini¹⁷⁹, F. Paige²⁷, G. Palacino⁶⁴, S. Palazzo^{40a,40b}, S. Palestini³², M. Palka^{41b}, D. Pallin³⁷, E. St. Panagiotopoulou¹⁰, I. Panagoulas¹⁰, C.E. Pandini⁵², J.G. Panduro Vazquez⁸⁰, P. Pani³², S. Panitkin²⁷, D. Pantea^{28b}, L. Paolozzi⁵², Th.D. Papadopoulou¹⁰, K. Papageorgiou^{9,s}, A. Paramonov⁶, D. Paredes Hernandez¹⁷⁹, A.J. Parker⁷⁵, M.A. Parker³⁰, K.A. Parker⁴⁵, F. Parodi^{53a,53b}, J.A. Parsons³⁸, U. Parzefall⁵¹, V.R. Pascuzzi¹⁶¹, J.M. Pasner¹³⁹, E. Pasqualucci^{134a}, S. Passaggio^{53a}, Fr. Pastore⁸⁰, S. Patariaia⁸⁶, J.R. Pater⁸⁷, T. Pauly³², B. Pearson¹⁰³, S. Pedraza Lopez¹⁷⁰, R. Pedro^{128a,128b}, S.V. Peleganchuk^{111,c}, O. Penc¹²⁹, C. Peng^{35a}, H. Peng^{36a}, J. Penwell⁶⁴, B.S. Peralva^{26b}, M.M. Perego¹³⁸, D.V. Perepelitsa²⁷, F. Peri¹⁷, L. Perini^{94a,94b}, H. Pernegger³², S. Perrella^{106a,106b}, R. Peschke⁴⁵, V.D. Peshekhonov^{68,*}, K. Peters⁴⁵, R.F.Y. Peters⁸⁷, B.A. Petersen³², T.C. Petersen³⁹, E. Petit⁵⁸, A. Petridis¹, C. Petridou¹⁵⁶, P. Petroff¹¹⁹, E. Petrolo^{134a}, M. Petrov¹²², F. Petrucci^{136a,136b}, N.E. Pettersson⁸⁹, A. Peyaud¹³⁸, R. Pezoa^{34b}, F.H. Phillips⁹³, P.W. Phillips¹³³, G. Piacquadio¹⁵⁰, E. Pianori¹⁷³, A. Picazio⁸⁹, E. Piccaro⁷⁹, M.A. Pickering¹²², R. Piegaia²⁹, J.E. Pilcher³³, A.D. Pilkington⁸⁷, M. Pinamonti^{135a,135b}, J.L. Pinfold³, H. Pirumov⁴⁵,

M. Pitt¹⁷⁵, L. Plazak^{146a}, M.-A. Pleier²⁷, V. Pleskot⁸⁶, E. Plotnikova⁶⁸, D. Pluth⁶⁷, P. Podberezko¹¹¹, R. Poettgen⁸⁴, R. Poggi^{123a,123b}, L. Poggioli¹¹⁹, I. Pogrebnyak⁹³, D. Pohl²³, I. Pokharel⁵⁷, G. Polesello^{123a}, A. Poley⁴⁵, A. Policicchio^{40a,40b}, R. Polifka³², A. Polini^{22a}, C.S. Pollard⁵⁶, V. Polychronakos²⁷, K. Pommès³², D. Ponomarenko¹⁰⁰, L. Pontecorvo^{134a}, G.A. Popeneciu^{28d}, D.M. Portillo Quintero⁸³, S. Pospisil¹³⁰, K. Potamianos⁴⁵, I.N. Potrap⁶⁸, C.J. Potter³⁰, H. Potti¹¹, T. Poulsen⁸⁴, J. Poveda³², M.E. Pozo Astigarraga³², P. Pralavorio⁸⁸, A. Pranko¹⁶, S. Prell⁶⁷, D. Price⁸⁷, M. Primavera^{76a}, S. Prince⁹⁰, N. Proklova¹⁰⁰, K. Prokofiev^{62c}, F. Prokoshin^{34b}, S. Protopopescu²⁷, J. Proudfoot⁶, M. Przybycien^{41a}, A. Puri¹⁶⁹, P. Puzo¹¹⁹, J. Qian⁹², G. Qin⁵⁶, Y. Qin⁸⁷, A. Quadt⁵⁷, M. Queitsch-Maitland⁴⁵, D. Quilty⁵⁶, S. Raddum¹²¹, V. Radeka²⁷, V. Radescu¹²², S.K. Radhakrishnan¹⁵⁰, P. Radloff¹¹⁸, P. Rados⁹¹, F. Ragusa^{94a,94b}, G. Rahal¹⁸¹, J.A. Raine⁸⁷, S. Rajagopalan²⁷, C. Rangel-Smith¹⁶⁸, T. Rashid¹¹⁹, S. Raspopov⁵, M.G. Ratti^{94a,94b}, D.M. Rauch⁴⁵, F. Rauscher¹⁰², S. Rave⁸⁶, I. Ravinovich¹⁷⁵, J.H. Rawling⁸⁷, M. Raymond³², A.L. Read¹²¹, N.P. Readioff⁵⁸, M. Reale^{76a,76b}, D.M. Rebuffi^{123a,123b}, A. Redelbach¹⁷⁷, G. Redlinger²⁷, R. Reece¹³⁹, R.G. Reed^{147c}, K. Reeves⁴⁴, L. Rehnisch¹⁷, J. Reichert¹²⁴, A. Reiss⁸⁶, C. Rembser³², H. Ren^{35a}, M. Rescigno^{134a}, S. Resconi^{94a}, E.D. Resseguie¹²⁴, S. Rettie¹⁷¹, E. Reynolds¹⁹, O.L. Rezanova^{111,c}, P. Reznicek¹³¹, R. Rezvani⁹⁷, R. Richter¹⁰³, S. Richter⁸¹, E. Richter-Was^{41b}, O. Ricken²³, M. Ridel⁸³, P. Rieck¹⁰³, C.J. Riegel¹⁷⁸, J. Rieger⁵⁷, O. Rifki¹¹⁵, M. Rijssenbeek¹⁵⁰, A. Rimoldi^{123a,123b}, M. Rimoldi¹⁸, L. Rinaldi^{22a}, G. Ripellino¹⁴⁹, B. Ristić³², E. Ritsch³², I. Riu¹³, F. Rizatdinova¹¹⁶, E. Rizvi⁷⁹, C. Rizzi¹³, R.T. Roberts⁸⁷, S.H. Robertson^{90,o}, A. Robichaud-Veronneau⁹⁰, D. Robinson³⁰, J.E.M. Robinson⁴⁵, A. Robson⁵⁶, E. Rocco⁸⁶, C. Roda^{126a,126b}, Y. Rodina^{88,al}, S. Rodriguez Bosca¹⁷⁰, A. Rodriguez Perez¹³, D. Rodriguez Rodriguez¹⁷⁰, S. Roe³², C.S. Rogan⁵⁹, O. Röhne¹²¹, J. Roloff⁵⁹, A. Romaniouk¹⁰⁰, M. Romano^{22a,22b}, S.M. Romano Saez³⁷, E. Romero Adam¹⁷⁰, N. Rompotis⁷⁷, M. Ronzani⁵¹, L. Roos⁸³, S. Rosati^{134a}, K. Rosbach⁵¹, P. Rose¹³⁹, N.-A. Rosien⁵⁷, E. Rossi^{106a,106b}, L.P. Rossi^{53a}, J.H.N. Rosten³⁰, R. Rosten¹⁴⁰, M. Rotaru^{28b}, J. Rothberg¹⁴⁰, D. Rousseau¹¹⁹, A. Rozanov⁸⁸, Y. Rozen¹⁵⁴, X. Ruan^{147c}, F. Rubbo¹⁴⁵, F. Rühr⁵¹, A. Ruiz-Martinez³¹, Z. Rurikova⁵¹, N.A. Rusakovitch⁶⁸, H.L. Russell⁹⁰, J.P. Rutherford⁷, N. Ruthmann³², Y.F. Ryabov¹²⁵, M. Rybar¹⁶⁹, G. Rybkin¹¹⁹, S. Ryu⁶, A. Ryzhov¹³², G.F. Rzehorz⁵⁷, A.F. Saavedra¹⁵², G. Sabato¹⁰⁹, S. Sacerdoti²⁹, H.F.-W. Sadrozinski¹³⁹, R. Sadykov⁶⁸, F. Safai Tehrani^{134a}, P. Saha¹¹⁰, M. Sahinsoy^{60a}, M. Saimpert⁴⁵, M. Saito¹⁵⁷, T. Saito¹⁵⁷, H. Sakamoto¹⁵⁷, Y. Sakurai¹⁷⁴, G. Salamanna^{136a,136b}, J.E. Salazar Loyola^{34b}, D. Salek¹⁰⁹, P.H. Sales De Bruin¹⁶⁸, D. Salihagic¹⁰³, A. Salnikov¹⁴⁵, J. Salt¹⁷⁰, D. Salvatore^{40a,40b}, F. Salvatore¹⁵¹, A. Salvucci^{62a,62b,62c}, A. Salzburger³², D. Sammel⁵¹, D. Sampsonidis¹⁵⁶, D. Sampsonidou¹⁵⁶, J. Sánchez¹⁷⁰, V. Sanchez Martinez¹⁷⁰, A. Sanchez Pineda^{167a,167c}, H. Sandaker¹²¹, R.L. Sandbach⁷⁹, C.O. Sander⁴⁵, M. Sandhoff¹⁷⁸, C. Sandoval²¹, D.P.C. Sankey¹³³, M. Sannino^{53a,53b}, Y. Sano¹⁰⁵, A. Sansoni⁵⁰, C. Santoni³⁷, H. Santos^{128a}, I. Santoyo Castillo¹⁵¹, A. Sapronov⁶⁸, J.G. Saraiva^{128a,128d}, B. Sarrazin²³, O. Sasaki⁶⁹, K. Sato¹⁶⁴, E. Sauvan⁵, G. Savage⁸⁰, P. Savard^{161,d}, N. Savic¹⁰³, C. Sawyer¹³³, L. Sawyer^{82,u}, J. Saxon³³, C. Sbarra^{22a}, A. Sbrizzi^{22a,22b}, T. Scanlon⁸¹, D.A. Scannicchio¹⁶⁶, J. Schaarschmidt¹⁴⁰, P. Schacht¹⁰³, B.M. Schachtner¹⁰², D. Schaefer³³, L. Schaefer¹²⁴, R. Schaefer⁴⁵, J. Schaeffer⁸⁶, S. Schaepe²³, S. Schaetzel^{60b}, U. Schäfer⁸⁶, A.C. Schaffer¹¹⁹, D. Schaile¹⁰², R.D. Schamberger¹⁵⁰, V.A. Schegelsky¹²⁵, D. Scheirich¹³¹, M. Schernau¹⁶⁶, C. Schiavi^{53a,53b}, S. Schier¹³⁹, L.K. Schildgen²³, C. Schillo⁵¹, M. Schioppa^{40a,40b}, S. Schlenker³², K.R. Schmidt-Sommerfeld¹⁰³, K. Schmieden³², C. Schmitt⁸⁶, S. Schmitt⁴⁵, S. Schmitz⁸⁶, U. Schnoor⁵¹, L. Schoeffel¹³⁸, A. Schoening^{60b}, B.D. Schoenrock⁹³, E. Schopf²³, M. Schott⁸⁶, J.F.P. Schouwenberg¹⁰⁸, J. Schovancova³², S. Schramm⁵², N. Schuh⁸⁶, A. Schulte⁸⁶, M.J. Schultens²³, H.-C. Schultz-Coulon^{60a}, H. Schulz¹⁷, M. Schumacher⁵¹, B.A. Schumm¹³⁹, Ph. Schune¹³⁸, A. Schwartzman¹⁴⁵, T.A. Schwarz⁹², H. Schweiger⁸⁷, Ph. Schwemling¹³⁸, R. Schwienhorst⁹³, J. Schwindling¹³⁸, A. Sciandra²³, G. Sciolla²⁵, M. Scornajenghi^{40a,40b}, F. Scuri^{126a,126b}, F. Scutti⁹¹, J. Searcy⁹², P. Seema²³, S.C. Seidel¹⁰⁷, A. Seiden¹³⁹, J.M. Seixas^{26a}, G. Sekhniaidze^{106a}, K. Sekhon⁹², S.J. Sekula⁴³, N. Semprini-Cesari^{22a,22b}, S. Senkin³⁷, C. Serfon¹²¹, L. Serin¹¹⁹, L. Serkin^{167a,167b}, M. Sessa^{136a,136b}, R. Seuster¹⁷², H. Severini¹¹⁵, T. Sfiligoi⁷⁸, F. Sforza¹⁶⁵, A. Sfyrla⁵², E. Shabalina⁵⁷, N.W. Shaikh^{148a,148b}, L.Y. Shan^{35a}, R. Shang¹⁶⁹, J.T. Shank²⁴, M. Shapiro¹⁶, P.B. Shatalov⁹⁹, K. Shaw^{167a,167b}, S.M. Shaw⁸⁷, A. Shcherbakova^{148a,148b}, C.Y. Shehu¹⁵¹, Y. Shen¹¹⁵, N. Sherafati³¹, P. Sherwood⁸¹, L. Shi^{153,am}, S. Shimizu⁷⁰, C.O. Shimmin¹⁷⁹, M. Shimojima¹⁰⁴, I.P.J. Shipsey¹²², S. Shirabe⁷³, M. Shiyakova^{68,an}, J. Shlomi¹⁷⁵, A. Shmeleva⁹⁸, D. Shoaleh Saadi⁹⁷,

M.J. Shochet³³, S. Shojaii^{94a,94b}, D.R. Shope¹¹⁵, S. Shrestha¹¹³, E. Shulga¹⁰⁰, M.A. Shupe⁷, P. Sicho¹²⁹, A.M. Sickles¹⁶⁹, P.E. Sidebo¹⁴⁹, E. Sideras Haddad^{147c}, O. Sidiropoulou¹⁷⁷, A. Sidoti^{22a,22b}, F. Siegert⁴⁷, Dj. Sijacki¹⁴, J. Silva^{128a,128d}, S.B. Silverstein^{148a}, V. Simak¹³⁰, L. Simic⁶⁸, S. Simion¹¹⁹, E. Simioni⁸⁶, B. Simmons⁸¹, M. Simon⁸⁶, P. Sinervo¹⁶¹, N.B. Sinev¹¹⁸, M. Sioli^{22a,22b}, G. Siragusa¹⁷⁷, I. Siral⁹², S.Yu. Sivoklokov¹⁰¹, J. Sjölin^{148a,148b}, M.B. Skinner⁷⁵, P. Skubic¹¹⁵, M. Slater¹⁹, T. Slavicek¹³⁰, M. Slawinska⁴², K. Sliwa¹⁶⁵, R. Slovak¹³¹, V. Smakhtin¹⁷⁵, B.H. Smart⁵, J. Smiesko^{146a}, N. Smirnov¹⁰⁰, S.Yu. Smirnov¹⁰⁰, Y. Smirnov¹⁰⁰, L.N. Smirnova^{101,ao}, O. Smirnova⁸⁴, J.W. Smith⁵⁷, M.N.K. Smith³⁸, R.W. Smith³⁸, M. Smizanska⁷⁵, K. Smolek¹³⁰, A.A. Snesarev⁹⁸, I.M. Snyder¹¹⁸, S. Snyder²⁷, R. Sobie^{172,o}, F. Socher⁴⁷, A. Soffer¹⁵⁵, A. Søgaard⁴⁹, D.A. Soh¹⁵³, G. Sokhrannyi⁷⁸, C.A. Solans Sanchez³², M. Solar¹³⁰, E.Yu. Soldatov¹⁰⁰, U. Soldevila¹⁷⁰, A.A. Solodkov¹³², A. Soloshenko⁶⁸, O.V. Solovyanov¹³², V. Solovyev¹²⁵, P. Sommer⁵¹, H. Son¹⁶⁵, A. Sopczak¹³⁰, D. Sosa^{60b}, C.L. Sotiropoulou^{126a,126b}, S. Sottocornola^{123a,123b}, R. Soualah^{167a,167c}, A.M. Soukharev^{111,c}, D. South⁴⁵, B.C. Sowden⁸⁰, S. Spagnolo^{76a,76b}, M. Spalla^{126a,126b}, M. Spangenberg¹⁷³, F. Spanò⁸⁰, D. Sperlich¹⁷, F. Spettel¹⁰³, T.M. Spieker^{60a}, R. Spighi^{22a}, G. Spigo³², L.A. Spiller⁹¹, M. Spousta¹³¹, R.D. St. Denis^{56,*}, A. Stabile^{94a}, R. Stamen^{60a}, S. Stamm¹⁷, E. Stanecka⁴², R.W. Stanek⁶, C. Stancu^{136a}, M.M. Stanitzki⁴⁵, B.S. Stapf¹⁰⁹, S. Stapnes¹²¹, E.A. Starchenko¹³², G.H. Stark³³, J. Stark⁵⁸, S.H. Stark³⁹, P. Staroba¹²⁹, P. Starovoitov^{60a}, S. Stärz³², R. Staszewski⁴², M. Stegler⁴⁵, P. Steinberg²⁷, B. Stelzer¹⁴⁴, H.J. Stelzer³², O. Stelzer-Chilton^{163a}, H. Stenzel⁵⁵, G.A. Stewart⁵⁶, M.C. Stockton¹¹⁸, M. Stoebe⁹⁰, G. Stoica^{28b}, P. Stolte⁵⁷, S. Stonjek¹⁰³, A.R. Stradling⁸, A. Straessner⁴⁷, M.E. Stramaglia¹⁸, J. Strandberg¹⁴⁹, S. Strandberg^{148a,148b}, M. Strauss¹¹⁵, P. Strizenec^{146b}, R. Ströhmer¹⁷⁷, D.M. Strom¹¹⁸, R. Stroynowski⁴³, A. Strubig⁴⁹, S.A. Stucci²⁷, B. Stugu¹⁵, N.A. Styles⁴⁵, D. Su¹⁴⁵, J. Su¹²⁷, S. Suchek^{60a}, Y. Sugaya¹²⁰, M. Suk¹³⁰, V.V. Sulin⁹⁸, DMS Sultan^{162a,162b}, S. Sultansoy^{4c}, T. Sumida⁷¹, S. Sun⁵⁹, X. Sun³, K. Suruliz¹⁵¹, C.J.E. Suster¹⁵², M.R. Sutton¹⁵¹, S. Suzuki⁶⁹, M. Svatos¹²⁹, M. Swiatlowski³³, S.P. Swift², I. Sykora^{146a}, T. Sykora¹³¹, D. Ta⁵¹, K. Tackmann⁴⁵, J. Taenzer¹⁵⁵, A. Taffard¹⁶⁶, R. Tahirout^{163a}, E. Tahirovic⁷⁹, N. Taiblum¹⁵⁵, H. Takai²⁷, R. Takashima⁷², E.H. Takasugi¹⁰³, K. Takeda⁷⁰, T. Takeshita¹⁴², Y. Takubo⁶⁹, M. Talby⁸⁸, A.A. Talyshev^{111,c}, J. Tanaka¹⁵⁷, M. Tanaka¹⁵⁹, R. Tanaka¹¹⁹, S. Tanaka⁶⁹, R. Tanioka⁷⁰, B.B. Tannenwald¹¹³, S. Tapia Araya^{34b}, S. Tapprogge⁸⁶, S. Tarem¹⁵⁴, G.F. Tartarelli^{94a}, P. Tas¹³¹, M. Tasevsky¹²⁹, T. Tashiro⁷¹, E. Tassi^{40a,40b}, A. Tavares Delgado^{128a,128b}, Y. Tayalati^{137e}, A.C. Taylor¹⁰⁷, A.J. Taylor⁴⁹, G.N. Taylor⁹¹, P.T.E. Taylor⁹¹, W. Taylor^{163b}, P. Teixeira-Dias⁸⁰, D. Temple¹⁴⁴, H. Ten Kate³², P.K. Teng¹⁵³, J.J. Teoh¹²⁰, F. Tepel¹⁷⁸, S. Terada⁶⁹, K. Terashi¹⁵⁷, J. Terron⁸⁵, S. Terzo¹³, M. Testa⁵⁰, R.J. Teuscher^{161,o}, T. Theveneaux-Pelzer⁸⁸, F. Thiele³⁹, J.P. Thomas¹⁹, J. Thomas-Wilsker⁸⁰, P.D. Thompson¹⁹, A.S. Thompson⁵⁶, L.A. Thomsen¹⁷⁹, E. Thomson¹²⁴, Y. Tian³⁸, M.J. Tibbetts¹⁶, R.E. Ticse Torres⁸⁸, V.O. Tikhomirov^{98,ap}, Yu.A. Tikhonov^{111,c}, S. Timoshenko¹⁰⁰, P. Tipton¹⁷⁹, S. Tisserant⁸⁸, K. Todome¹⁵⁹, S. Todorova-Nova⁵, S. Todt⁴⁷, J. Tojo⁷³, S. Tokár^{146a}, K. Tokushuku⁶⁹, E. Tolley⁵⁹, L. Tomlinson⁸⁷, M. Tomoto¹⁰⁵, L. Tompkins^{145,aq}, K. Toms¹⁰⁷, B. Tong⁵⁹, P. Tornambe⁵¹, E. Torrence¹¹⁸, H. Torres⁴⁷, E. Torró Pastor¹⁴⁰, J. Toth^{88,ar}, F. Touchard⁸⁸, D.R. Tovey¹⁴¹, C.J. Treado¹¹², T. Trefzger¹⁷⁷, F. Tresoldi¹⁵¹, A. Tricoli²⁷, I.M. Trigger^{163a}, S. Trincas-Duvoid⁸³, M.F. Tripiana¹³, W. Trischuk¹⁶¹, B. Trocmé⁵⁸, A. Trofymov⁴⁵, C. Troncon^{94a}, M. Trottier-McDonald¹⁶, M. Trovatelli¹⁷², L. Truong^{147b}, M. Trzebinski⁴², A. Trzupek⁴², K.W. Tsang^{62a}, J.C.-L. Tseng¹²², P.V. Tsiarehsha⁹⁵, G. Tsipolitis¹⁰, N. Tsirintanis⁹, S. Tsiskaridze¹³, V. Tsiskaridze⁵¹, E.G. Tskhadadze^{54a}, I.I. Tsukerman⁹⁹, V. Tsulaia¹⁶, S. Tsuno⁶⁹, D. Tsybychev¹⁵⁰, Y. Tu^{62b}, A. Tudorache^{28b}, V. Tudorache^{28b}, T.T. Tulbure^{28a}, A.N. Tuna⁵⁹, S. Turchikhin⁶⁸, D. Turgeman¹⁷⁵, I. Turk Cakir^{4b,as}, R. Turra^{94a}, P.M. Tuts³⁸, G. Uccielli^{22a,22b}, I. Ueda⁶⁹, M. Ughetto^{148a,148b}, F. Ukegawa¹⁶⁴, G. Unal³², A. Undrus²⁷, G. Unel¹⁶⁶, F.C. Ungaro⁹¹, Y. Unno⁶⁹, K. Uno¹⁵⁷, C. Unverdorben¹⁰², J. Urban^{146b}, P. Urquijo⁹¹, P. Urrejola⁸⁶, G. Usai⁸, J. Usui⁶⁹, L. Vacavant⁸⁸, V. Vacek¹³⁰, B. Vachon⁹⁰, K.O.H. Vadla¹²¹, A. Vaidya⁸¹, C. Valderanis¹⁰², E. Valdes Santurio^{148a,148b}, M. Valente⁵², S. Valentini^{22a,22b}, A. Valero¹⁷⁰, L. Valéry¹³, S. Valkar¹³¹, A. Vallier⁵, J.A. Valls Ferrer¹⁷⁰, W. Van Den Wollenberg¹⁰⁹, H. van der Graaf¹⁰⁹, P. van Gemmeren⁶, J. Van Nieuwkoop¹⁴⁴, I. van Vulpen¹⁰⁹, M.C. van Woerden¹⁰⁹, M. Vanadia^{135a,135b}, W. Vandelli³², A. Vaniachine¹⁶⁰, P. Vankov¹⁰⁹, G. Vardanyan¹⁸⁰, R. Vari^{134a}, E.W. Varnes⁷, C. Varni^{53a,53b}, T. Varol⁴³, D. Varouchas¹¹⁹, A. Vartapetian⁸, K.E. Varvell¹⁵², J.G. Vasquez¹⁷⁹, G.A. Vasquez^{34b}, F. Vazeille³⁷, D. Vazquez Furelos¹³, T. Vazquez Schroeder⁹⁰, J. Veatch⁵⁷, V. Veeraraghavan⁷, L.M. Veloce¹⁶¹, F. Veloso^{128a,128c}, S. Veneziano^{134a}, A. Ventura^{76a,76b},

M. Venturi¹⁷², N. Venturi³², A. Venturini²⁵, V. Vercesi^{123a}, M. Verducci^{136a,136b}, W. Verkerke¹⁰⁹, A.T. Vermeulen¹⁰⁹, J.C. Vermeulen¹⁰⁹, M.C. Vetterli^{144,d}, N. Viaux Maira^{34b}, O. Viazlo⁸⁴, I. Vichou^{169,*}, T. Vickey¹⁴¹, O.E. Vickey Boeriu¹⁴¹, G.H.A. Viehhauser¹²², S. Viel¹⁶, L. Vigani¹²², M. Villa^{22a,22b}, M. Villaplana Perez^{94a,94b}, E. Vilucchi⁵⁰, M.G. Vincet³¹, V.B. Vinogradov⁶⁸, A. Vishwakarma⁴⁵, C. Vittori^{22a,22b}, I. Vivarelli¹⁵¹, S. Vlachos¹⁰, M. Vogel¹⁷⁸, P. Vokac¹³⁰, G. Volpi¹³, H. von der Schmitt¹⁰³, E. von Toerne²³, V. Vorobel¹³¹, K. Vorobev¹⁰⁰, M. Vos¹⁷⁰, R. Voss³², J.H. Vosseveld⁷⁷, N. Vranjes¹⁴, M. Vranjes Milosavljevic¹⁴, V. Vrba¹³⁰, M. Vreeswijk¹⁰⁹, R. Vuillermet³², I. Vukotic³³, P. Wagner²³, W. Wagner¹⁷⁸, J. Wagner-Kuhr¹⁰², H. Wahlberg⁷⁴, S. Wahrmond⁴⁷, J. Walder⁷⁵, R. Walker¹⁰², W. Walkowiak¹⁴³, V. Wallangen^{148a,148b}, C. Wang^{35b}, C. Wang^{36b,at}, F. Wang¹⁷⁶, H. Wang¹⁶, H. Wang³, J. Wang⁴⁵, J. Wang¹⁵², Q. Wang¹¹⁵, R.-J. Wang⁸³, R. Wang⁶, S.M. Wang¹⁵³, T. Wang³⁸, W. Wang^{153,au}, W. Wang^{36a,av}, Z. Wang^{36c}, C. Wanotayaroj⁴⁵, A. Warburton⁹⁰, C.P. Ward³⁰, D.R. Wardrope⁸¹, A. Washbrook⁴⁹, P.M. Watkins¹⁹, A.T. Watson¹⁹, M.F. Watson¹⁹, G. Watts¹⁴⁰, S. Watts⁸⁷, B.M. Waugh⁸¹, A.F. Webb¹¹, S. Webb⁸⁶, M.S. Weber¹⁸, S.M. Weber^{60a}, S.W. Weber¹⁷⁷, S.A. Weber³¹, J.S. Webster⁶, A.R. Weidberg¹²², B. Weinert⁶⁴, J. Weingarten⁵⁷, M. Weirich⁸⁶, C. Weiser⁵¹, H. Weits¹⁰⁹, P.S. Wells³², T. Wenaus²⁷, T. Wengler³², S. Wenig³², N. Wermes²³, M.D. Werner⁶⁷, P. Werner³², M. Wessels^{60a}, T.D. Weston¹⁸, K. Whalen¹¹⁸, N.L. Whallon¹⁴⁰, A.M. Wharton⁷⁵, A.S. White⁹², A. White⁸, M.J. White¹, R. White^{34b}, D. Whiteson¹⁶⁶, B.W. Whitmore⁷⁵, F.J. Wickens¹³³, W. Wiedenmann¹⁷⁶, M. Wielers¹³³, C. Wiglesworth³⁹, L.A.M. Wiik-Fuchs⁵¹, A. Wildauer¹⁰³, F. Wilk⁸⁷, H.G. Wilkens³², H.H. Williams¹²⁴, S. Williams¹⁰⁹, C. Willis⁹³, S. Willocq⁸⁹, J.A. Wilson¹⁹, I. Wingerter-Seez⁵, E. Winkels¹⁵¹, F. Winklmeier¹¹⁸, O.J. Winston¹⁵¹, B.T. Winter²³, M. Wittgen¹⁴⁵, M. Wobisch^{82,u}, T.M.H. Wolf¹⁰⁹, R. Wolff⁸⁸, M.W. Wolter⁴², H. Wolters^{128a,128c}, V.W.S. Wong¹⁷¹, N.L. Woods¹³⁹, S.D. Worm¹⁹, B.K. Wosiek⁴², J. Wotschack³², K.W. Wozniak⁴², M. Wu³³, S.L. Wu¹⁷⁶, X. Wu⁵², Y. Wu⁹², T.R. Wyatt⁸⁷, B.M. Wynne⁴⁹, S. Xella³⁹, Z. Xi⁹², L. Xia^{35c}, D. Xu^{35a}, L. Xu²⁷, T. Xu¹³⁸, B. Yabsley¹⁵², S. Yacoob^{147a}, D. Yamaguchi¹⁵⁹, Y. Yamaguchi¹⁵⁹, A. Yamamoto⁶⁹, S. Yamamoto¹⁵⁷, T. Yamanaka¹⁵⁷, F. Yamane⁷⁰, M. Yamatani¹⁵⁷, Y. Yamazaki⁷⁰, Z. Yan²⁴, H. Yang^{36c}, H. Yang¹⁶, Y. Yang¹⁵³, Z. Yang¹⁵, W.-M. Yao¹⁶, Y.C. Yap⁴⁵, Y. Yasu⁶⁹, E. Yatsenko⁵, K.H. Yau Wong²³, J. Ye⁴³, S. Ye²⁷, I. Yeletsikh⁶⁸, E. Yigitbasi²⁴, E. Yildirim⁸⁶, K. Yorita¹⁷⁴, K. Yoshihara¹²⁴, C. Young¹⁴⁵, C.J.S. Young³², J. Yu⁸, J. Yu⁶⁷, S.P.Y. Yuen²³, I. Yusuff^{30,aw}, B. Zabinski⁴², G. Zacharis¹⁰, R. Zaidan¹³, A.M. Zaitsev^{132,aj}, N. Zakharchuk⁴⁵, J. Zalieckas¹⁵, A. Zaman¹⁵⁰, S. Zambito⁵⁹, D. Zanzi⁹¹, C. Zeitnitz¹⁷⁸, G. Zemaityte¹²², A. Zemla^{41a}, J.C. Zeng¹⁶⁹, Q. Zeng¹⁴⁵, O. Zenin¹³², T. Ženiš^{146a}, D. Zerwas¹¹⁹, D. Zhang^{36b}, D. Zhang⁹², F. Zhang¹⁷⁶, G. Zhang^{36a,av}, H. Zhang¹¹⁹, J. Zhang⁶, L. Zhang⁵¹, L. Zhang^{36a}, M. Zhang¹⁶⁹, P. Zhang^{35b}, R. Zhang²³, R. Zhang^{36a,at}, X. Zhang^{36b}, Y. Zhang^{35a}, Z. Zhang¹¹⁹, X. Zhao⁴³, Y. Zhao^{36b,ax}, Z. Zhao^{36a}, A. Zhemchugov⁶⁸, B. Zhou⁹², C. Zhou¹⁷⁶, L. Zhou⁴³, M. Zhou^{35a}, M. Zhou¹⁵⁰, N. Zhou^{35c}, C.G. Zhu^{36b}, H. Zhu^{35a}, J. Zhu⁹², Y. Zhu^{36a}, X. Zhuang^{35a}, K. Zhukov⁹⁸, A. Zibell¹⁷⁷, D. Zieminska⁶⁴, N.I. Zimine⁶⁸, C. Zimmermann⁸⁶, S. Zimmermann⁵¹, Z. Zinonos¹⁰³, M. Zinser⁸⁶, M. Ziolkowski¹⁴³, L. Živković¹⁴, G. Zobernig¹⁷⁶, A. Zoccoli^{22a,22b}, R. Zou³³, M. zur Nedden¹⁷, L. Zwalinski³²

¹ Department of Physics, University of Adelaide, Adelaide, Australia

² Physics Department, SUNY Albany, Albany, NY, United States

³ Department of Physics, University of Alberta, Edmonton, AB, Canada

⁴ (a) Department of Physics, Ankara University, Ankara; (b) Istanbul Aydin University, Istanbul; (c) Division of Physics, TOBB University of Economics and Technology, Ankara, Turkey

⁵ LAPP, CNRS/IN2P3 and Université Savoie Mont Blanc, Annecy-le-Vieux, France

⁶ High Energy Physics Division, Argonne National Laboratory, Argonne, IL, United States

⁷ Department of Physics, University of Arizona, Tucson, AZ, United States

⁸ Department of Physics, The University of Texas at Arlington, Arlington, TX, United States

⁹ Physics Department, National and Kapodistrian University of Athens, Athens, Greece

¹⁰ Physics Department, National Technical University of Athens, Zografou, Greece

¹¹ Department of Physics, The University of Texas at Austin, Austin, TX, United States

¹² Institute of Physics, Azerbaijan Academy of Sciences, Baku, Azerbaijan

¹³ Institut de Física d'Altes Energies (IFAE), The Barcelona Institute of Science and Technology, Barcelona, Spain

¹⁴ Institute of Physics, University of Belgrade, Belgrade, Serbia

¹⁵ Department for Physics and Technology, University of Bergen, Bergen, Norway

¹⁶ Physics Division, Lawrence Berkeley National Laboratory and University of California, Berkeley, CA, United States

¹⁷ Department of Physics, Humboldt University, Berlin, Germany

¹⁸ Albert Einstein Center for Fundamental Physics and Laboratory for High Energy Physics, University of Bern, Bern, Switzerland

¹⁹ School of Physics and Astronomy, University of Birmingham, Birmingham, United Kingdom

²⁰ (a) Department of Physics, Bogazici University, Istanbul; (b) Department of Physics Engineering, Gaziantep University, Gaziantep; (d) Istanbul Bilgi University, Faculty of Engineering and Natural Sciences, Istanbul; (e) Bahcesehir University, Faculty of Engineering and Natural Sciences, Istanbul, Turkey

²¹ Centro de Investigaciones, Universidad Antonio Narino, Bogota, Colombia

²² (a) INFN Sezione di Bologna; (b) Dipartimento di Fisica e Astronomia, Università di Bologna, Bologna, Italy

²³ Physikalisches Institut, University of Bonn, Bonn, Germany

- ²⁴ Department of Physics, Boston University, Boston, MA, United States
- ²⁵ Department of Physics, Brandeis University, Waltham, MA, United States
- ²⁶ ^(a) Universidade Federal do Rio De Janeiro COPPE/EE/IF, Rio de Janeiro; ^(b) Electrical Circuits Department, Federal University of Juiz de Fora (UFJF), Juiz de Fora; ^(c) Federal University of Sao Joao del Rei (UFSJ), Sao Joao del Rei; ^(d) Instituto de Fisica, Universidade de Sao Paulo, Sao Paulo, Brazil
- ²⁷ Physics Department, Brookhaven National Laboratory, Upton, NY, United States
- ²⁸ ^(a) Transilvania University of Brasov, Brasov; ^(b) Horia Hulubei National Institute of Physics and Nuclear Engineering, Bucharest; ^(c) Department of Physics, Alexandru Ioan Cuza University of Iasi, Iasi; ^(d) National Institute for Research and Development of Isotopic and Molecular Technologies, Physics Department, Cluj Napoca; ^(e) University Politehnica Bucharest, Bucharest; ^(f) West University in Timisoara, Timisoara, Romania
- ²⁹ Departamento de Física, Universidad de Buenos Aires, Buenos Aires, Argentina
- ³⁰ Cavendish Laboratory, University of Cambridge, Cambridge, United Kingdom
- ³¹ Department of Physics, Carleton University, Ottawa, ON, Canada
- ³² CERN, Geneva, Switzerland
- ³³ Enrico Fermi Institute, University of Chicago, Chicago, IL, United States
- ³⁴ ^(a) Departamento de Física, Pontificia Universidad Católica de Chile, Santiago; ^(b) Departamento de Física, Universidad Técnica Federico Santa María, Valparaíso, Chile
- ³⁵ ^(a) Institute of High Energy Physics, Chinese Academy of Sciences, Beijing; ^(b) Department of Physics, Nanjing University, Jiangsu; ^(c) Physics Department, Tsinghua University, Beijing 100084, China
- ³⁶ ^(a) Department of Modern Physics and State Key Laboratory of Particle Detection and Electronics, University of Science and Technology of China, Anhui; ^(b) School of Physics, Shandong University, Shandong; ^(c) Department of Physics and Astronomy, Key Laboratory for Particle Physics, Astrophysics and Cosmology, Ministry of Education; Shanghai Key Laboratory for Particle Physics and Cosmology, Shanghai Jiao Tong University, Shanghai (also at PKU-CHEP), China
- ³⁷ Université Clermont Auvergne, CNRS/IN2P3, LPC, Clermont-Ferrand, France
- ³⁸ Nevis Laboratory, Columbia University, Irvington, NY, United States
- ³⁹ Niels Bohr Institute, University of Copenhagen, Copenhagen, Denmark
- ⁴⁰ ^(a) INFN Gruppo Collegato di Cosenza, Laboratori Nazionali di Frascati; ^(b) Dipartimento di Fisica, Università della Calabria, Rende, Italy
- ⁴¹ ^(a) AGH University of Science and Technology, Faculty of Physics and Applied Computer Science, Krakow; ^(b) Marian Smoluchowski Institute of Physics, Jagiellonian University, Krakow, Poland
- ⁴² Institute of Nuclear Physics Polish Academy of Sciences, Krakow, Poland
- ⁴³ Physics Department, Southern Methodist University, Dallas, TX, United States
- ⁴⁴ Physics Department, University of Texas at Dallas, Richardson, TX, United States
- ⁴⁵ DESY, Hamburg and Zeuthen, Germany
- ⁴⁶ Lehrstuhl für Experimentelle Physik IV, Technische Universität Dortmund, Dortmund, Germany
- ⁴⁷ Institut für Kern- und Teilchenphysik, Technische Universität Dresden, Dresden, Germany
- ⁴⁸ Department of Physics, Duke University, Durham, NC, United States
- ⁴⁹ SUPA – School of Physics and Astronomy, University of Edinburgh, Edinburgh, United Kingdom
- ⁵⁰ INFN e Laboratori Nazionali di Frascati, Frascati, Italy
- ⁵¹ Fakultät für Mathematik und Physik, Albert-Ludwigs-Universität, Freiburg, Germany
- ⁵² Département de Physique Nucléaire et Corpusculaire, Université de Genève, Geneva, Switzerland
- ⁵³ ^(a) INFN Sezione di Genova; ^(b) Dipartimento di Fisica, Università di Genova, Genova, Italy
- ⁵⁴ ^(a) E. Andronikashvili Institute of Physics, Iv. Javakishvili Tbilisi State University, Tbilisi; ^(b) High Energy Physics Institute, Tbilisi State University, Tbilisi, Georgia
- ⁵⁵ II Physikalisches Institut, Justus-Liebig-Universität Giessen, Giessen, Germany
- ⁵⁶ SUPA – School of Physics and Astronomy, University of Glasgow, Glasgow, United Kingdom
- ⁵⁷ II Physikalisches Institut, Georg-August-Universität, Göttingen, Germany
- ⁵⁸ Laboratoire de Physique Subatomique et de Cosmologie, Université Grenoble-Alpes, CNRS/IN2P3, Grenoble, France
- ⁵⁹ Laboratory for Particle Physics and Cosmology, Harvard University, Cambridge, MA, United States
- ⁶⁰ ^(a) Kirchhoff-Institut für Physik, Ruprecht-Karls-Universität Heidelberg, Heidelberg; ^(b) Physikalisches Institut, Ruprecht-Karls-Universität Heidelberg, Heidelberg, Germany
- ⁶¹ Faculty of Applied Information Science, Hiroshima Institute of Technology, Hiroshima, Japan
- ⁶² ^(a) Department of Physics, The Chinese University of Hong Kong, Shatin, N.T., Hong Kong; ^(b) Department of Physics, The University of Hong Kong, Hong Kong; ^(c) Department of Physics and Institute for Advanced Study, The Hong Kong University of Science and Technology, Clear Water Bay, Kowloon, Hong Kong, China
- ⁶³ Department of Physics, National Tsing Hua University, Taiwan, Taiwan
- ⁶⁴ Department of Physics, Indiana University, Bloomington, IN, United States
- ⁶⁵ Institut für Astro- und Teilchenphysik, Leopold-Franzens-Universität, Innsbruck, Austria
- ⁶⁶ University of Iowa, Iowa City, IA, United States
- ⁶⁷ Department of Physics and Astronomy, Iowa State University, Ames, IA, United States
- ⁶⁸ Joint Institute for Nuclear Research, JINR Dubna, Dubna, Russia
- ⁶⁹ KEK, High Energy Accelerator Research Organization, Tsukuba, Japan
- ⁷⁰ Graduate School of Science, Kobe University, Kobe, Japan
- ⁷¹ Faculty of Science, Kyoto University, Kyoto, Japan
- ⁷² Kyoto University of Education, Kyoto, Japan
- ⁷³ Research Center for Advanced Particle Physics and Department of Physics, Kyushu University, Fukuoka, Japan
- ⁷⁴ Instituto de Física La Plata, Universidad Nacional de La Plata and CONICET, La Plata, Argentina
- ⁷⁵ Physics Department, Lancaster University, Lancaster, United Kingdom
- ⁷⁶ ^(a) INFN Sezione di Lecce; ^(b) Dipartimento di Matematica e Fisica, Università del Salento, Lecce, Italy
- ⁷⁷ Oliver Lodge Laboratory, University of Liverpool, Liverpool, United Kingdom
- ⁷⁸ Department of Experimental Particle Physics, Jožef Stefan Institute and Department of Physics, University of Ljubljana, Ljubljana, Slovenia
- ⁷⁹ School of Physics and Astronomy, Queen Mary University of London, London, United Kingdom
- ⁸⁰ Department of Physics, Royal Holloway University of London, Surrey, United Kingdom
- ⁸¹ Department of Physics and Astronomy, University College London, London, United Kingdom
- ⁸² Louisiana Tech University, Ruston, LA, United States
- ⁸³ Laboratoire de Physique Nucléaire et de Hautes Energies, UPMC and Université Paris-Diderot and CNRS/IN2P3, Paris, France
- ⁸⁴ Fysiska institutionen, Lunds universitet, Lund, Sweden
- ⁸⁵ Departamento de Física Teórica C-15, Universidad Autónoma de Madrid, Madrid, Spain
- ⁸⁶ Institut für Physik, Universität Mainz, Mainz, Germany
- ⁸⁷ School of Physics and Astronomy, University of Manchester, Manchester, United Kingdom
- ⁸⁸ CPPM, Aix-Marseille Université and CNRS/IN2P3, Marseille, France
- ⁸⁹ Department of Physics, University of Massachusetts, Amherst, MA, United States
- ⁹⁰ Department of Physics, McGill University, Montreal, QC, Canada
- ⁹¹ School of Physics, University of Melbourne, Victoria, Australia
- ⁹² Department of Physics, The University of Michigan, Ann Arbor, MI, United States
- ⁹³ Department of Physics and Astronomy, Michigan State University, East Lansing, MI, United States
- ⁹⁴ ^(a) INFN Sezione di Milano; ^(b) Dipartimento di Fisica, Università di Milano, Milano, Italy

- ⁹⁵ B.I. Stepanov Institute of Physics, National Academy of Sciences of Belarus, Minsk, Belarus
- ⁹⁶ Research Institute for Nuclear Problems of Byelorussian State University, Minsk, Belarus
- ⁹⁷ Group of Particle Physics, University of Montreal, Montreal, QC, Canada
- ⁹⁸ P.N. Lebedev Physical Institute of the Russian Academy of Sciences, Moscow, Russia
- ⁹⁹ Institute for Theoretical and Experimental Physics (ITEP), Moscow, Russia
- ¹⁰⁰ National Research Nuclear University MEPhI, Moscow, Russia
- ¹⁰¹ D.V. Skobeltsyn Institute of Nuclear Physics, M.V. Lomonosov Moscow State University, Moscow, Russia
- ¹⁰² Fakultät für Physik, Ludwig-Maximilians-Universität München, München, Germany
- ¹⁰³ Max-Planck-Institut für Physik (Werner-Heisenberg-Institut), München, Germany
- ¹⁰⁴ Nagasaki Institute of Applied Science, Nagasaki, Japan
- ¹⁰⁵ Graduate School of Science and Kobayashi-Maskawa Institute, Nagoya University, Nagoya, Japan
- ¹⁰⁶ ^(a) INFN Sezione di Napoli; ^(b) Dipartimento di Fisica, Università di Napoli, Napoli, Italy
- ¹⁰⁷ Department of Physics and Astronomy, University of New Mexico, Albuquerque, NM, United States
- ¹⁰⁸ Institute for Mathematics, Astrophysics and Particle Physics, Radboud University Nijmegen/Nikhef, Nijmegen, Netherlands
- ¹⁰⁹ Nikhef National Institute for Subatomic Physics and University of Amsterdam, Amsterdam, Netherlands
- ¹¹⁰ Department of Physics, Northern Illinois University, DeKalb, IL, United States
- ¹¹¹ Budker Institute of Nuclear Physics, SB RAS, Novosibirsk, Russia
- ¹¹² Department of Physics, New York University, New York, NY, United States
- ¹¹³ Ohio State University, Columbus, OH, United States
- ¹¹⁴ Faculty of Science, Okayama University, Okayama, Japan
- ¹¹⁵ Homer L. Dodge Department of Physics and Astronomy, University of Oklahoma, Norman, OK, United States
- ¹¹⁶ Department of Physics, Oklahoma State University, Stillwater, OK, United States
- ¹¹⁷ Palacký University, RCPTM, Olomouc, Czech Republic
- ¹¹⁸ Center for High Energy Physics, University of Oregon, Eugene, OR, United States
- ¹¹⁹ LAL, Univ. Paris-Sud, CNRS/IN2P3, Université Paris-Saclay, Orsay, France
- ¹²⁰ Graduate School of Science, Osaka University, Osaka, Japan
- ¹²¹ Department of Physics, University of Oslo, Oslo, Norway
- ¹²² Department of Physics, Oxford University, Oxford, United Kingdom
- ¹²³ ^(a) INFN Sezione di Pavia; ^(b) Dipartimento di Fisica, Università di Pavia, Pavia, Italy
- ¹²⁴ Department of Physics, University of Pennsylvania, Philadelphia, PA, United States
- ¹²⁵ National Research Centre "Kurchatov Institute", B.P. Konstantinov Petersburg Nuclear Physics Institute, St. Petersburg, Russia
- ¹²⁶ ^(a) INFN Sezione di Pisa; ^(b) Dipartimento di Fisica E. Fermi, Università di Pisa, Pisa, Italy
- ¹²⁷ Department of Physics and Astronomy, University of Pittsburgh, Pittsburgh, PA, United States
- ¹²⁸ ^(a) Laboratório de Instrumentação e Física Experimental de Partículas – LIP, Lisboa; ^(b) Faculdade de Ciências, Universidade de Lisboa, Lisboa; ^(c) Department of Physics, University of Coimbra, Coimbra; ^(d) Centro de Física Nuclear da Universidade de Lisboa, Lisboa; ^(e) Departamento de Física, Universidade do Minho, Braga; ^(f) Departamento de Física Teórica y del Cosmos, Universidad de Granada, Granada; ^(g) Dep Física and CEFITEC of Faculdade de Ciências e Tecnologia, Universidade Nova de Lisboa, Caparica, Portugal
- ¹²⁹ Institute of Physics, Academy of Sciences of the Czech Republic, Praha, Czech Republic
- ¹³⁰ Czech Technical University in Prague, Praha, Czech Republic
- ¹³¹ Charles University, Faculty of Mathematics and Physics, Prague, Czech Republic
- ¹³² State Research Center Institute for High Energy Physics (Protvino), NRC KI, Russia
- ¹³³ Particle Physics Department, Rutherford Appleton Laboratory, Didcot, United Kingdom
- ¹³⁴ ^(a) INFN Sezione di Roma; ^(b) Dipartimento di Fisica, Sapienza Università di Roma, Roma, Italy
- ¹³⁵ ^(a) INFN Sezione di Roma Tor Vergata; ^(b) Dipartimento di Fisica, Università di Roma Tor Vergata, Roma, Italy
- ¹³⁶ ^(a) INFN Sezione di Roma Tre; ^(b) Dipartimento di Matematica e Fisica, Università Roma Tre, Roma, Italy
- ¹³⁷ ^(a) Faculté des Sciences Ain Chock, Réseau Universitaire de Physique des Hautes Energies – Université Hassan II, Casablanca; ^(b) Centre National de l'Energie des Sciences Techniques Nucleaires, Rabat; ^(c) Faculté des Sciences Semlalia, Université Cadi Ayyad, LPHEA Marrakech; ^(d) Faculté des Sciences, Université Mohamed Premier and LPTPM, Oujda; ^(e) Faculté des sciences, Université Mohammed V, Rabat, Morocco
- ¹³⁸ DSM/IRFU (Institut de Recherches sur les Lois Fondamentales de l'Univers), CEA Saclay (Commissariat à l'Energie Atomique et aux Energies Alternatives), Gif-sur-Yvette, France
- ¹³⁹ Santa Cruz Institute for Particle Physics, University of California Santa Cruz, Santa Cruz, CA, United States
- ¹⁴⁰ Department of Physics, University of Washington, Seattle, WA, United States
- ¹⁴¹ Department of Physics and Astronomy, University of Sheffield, Sheffield, United Kingdom
- ¹⁴² Department of Physics, Shinshu University, Nagano, Japan
- ¹⁴³ Department Physik, Universität Siegen, Siegen, Germany
- ¹⁴⁴ Department of Physics, Simon Fraser University, Burnaby, BC, Canada
- ¹⁴⁵ SLAC National Accelerator Laboratory, Stanford, CA, United States
- ¹⁴⁶ ^(a) Faculty of Mathematics, Physics & Informatics, Comenius University, Bratislava; ^(b) Department of Subnuclear Physics, Institute of Experimental Physics of the Slovak Academy of Sciences, Kosice, Slovak Republic
- ¹⁴⁷ ^(a) Department of Physics, University of Cape Town, Cape Town; ^(b) Department of Physics, University of Johannesburg, Johannesburg; ^(c) School of Physics, University of the Witwatersrand, Johannesburg, South Africa
- ¹⁴⁸ ^(a) Department of Physics, Stockholm University; ^(b) The Oskar Klein Centre, Stockholm, Sweden
- ¹⁴⁹ Physics Department, Royal Institute of Technology, Stockholm, Sweden
- ¹⁵⁰ Departments of Physics & Astronomy and Chemistry, Stony Brook University, Stony Brook, NY, United States
- ¹⁵¹ Department of Physics and Astronomy, University of Sussex, Brighton, United Kingdom
- ¹⁵² School of Physics, University of Sydney, Sydney, Australia
- ¹⁵³ Institute of Physics, Academia Sinica, Taipei, Taiwan
- ¹⁵⁴ Department of Physics, Technion: Israel Institute of Technology, Haifa, Israel
- ¹⁵⁵ Raymond and Beverly Sackler School of Physics and Astronomy, Tel Aviv University, Tel Aviv, Israel
- ¹⁵⁶ Department of Physics, Aristotle University of Thessaloniki, Thessaloniki, Greece
- ¹⁵⁷ International Center for Elementary Particle Physics and Department of Physics, The University of Tokyo, Tokyo, Japan
- ¹⁵⁸ Graduate School of Science and Technology, Tokyo Metropolitan University, Tokyo, Japan
- ¹⁵⁹ Department of Physics, Tokyo Institute of Technology, Tokyo, Japan
- ¹⁶⁰ Tomsk State University, Tomsk, Russia
- ¹⁶¹ Department of Physics, University of Toronto, Toronto, ON, Canada
- ¹⁶² ^(a) INFN-TIFPA; ^(b) University of Trento, Trento, Italy
- ¹⁶³ ^(a) TRIUMF, Vancouver, BC; ^(b) Department of Physics and Astronomy, York University, Toronto, ON, Canada
- ¹⁶⁴ Faculty of Pure and Applied Sciences, and Center for Integrated Research in Fundamental Science and Engineering, University of Tsukuba, Tsukuba, Japan
- ¹⁶⁵ Department of Physics and Astronomy, Tufts University, Medford, MA, United States
- ¹⁶⁶ Department of Physics and Astronomy, University of California Irvine, Irvine, CA, United States
- ¹⁶⁷ ^(a) INFN Gruppo Collegato di Udine, Sezione di Trieste, Udine; ^(b) ICTP, Trieste; ^(c) Dipartimento di Chimica, Fisica e Ambiente, Università di Udine, Udine, Italy

- ¹⁶⁸ Department of Physics and Astronomy, University of Uppsala, Uppsala, Sweden
¹⁶⁹ Department of Physics, University of Illinois, Urbana, IL, United States
¹⁷⁰ Instituto de Física Corpuscular (IFIC), Centro Mixto Universidad de Valencia – CSIC, Spain
¹⁷¹ Department of Physics, University of British Columbia, Vancouver, BC, Canada
¹⁷² Department of Physics and Astronomy, University of Victoria, Victoria, BC, Canada
¹⁷³ Department of Physics, University of Warwick, Coventry, United Kingdom
¹⁷⁴ Waseda University, Tokyo, Japan
¹⁷⁵ Department of Particle Physics, The Weizmann Institute of Science, Rehovot, Israel
¹⁷⁶ Department of Physics, University of Wisconsin, Madison, WI, United States
¹⁷⁷ Fakultät für Physik und Astronomie, Julius-Maximilians-Universität, Würzburg, Germany
¹⁷⁸ Fakultät für Mathematik und Naturwissenschaften, Fachgruppe Physik, Bergische Universität Wuppertal, Wuppertal, Germany
¹⁷⁹ Department of Physics, Yale University, New Haven, CT, United States
¹⁸⁰ Yerevan Physics Institute, Yerevan, Armenia
¹⁸¹ Centre de Calcul de l'Institut National de Physique Nucléaire et de Physique des Particules (IN2P3), Villeurbanne, France
¹⁸² Academia Sinica Grid Computing, Institute of Physics, Academia Sinica, Taipei, Taiwan

- ^a Also at Department of Physics, King's College London, London, United Kingdom.
^b Also at Institute of Physics, Azerbaijan Academy of Sciences, Baku, Azerbaijan.
^c Also at Novosibirsk State University, Novosibirsk, Russia.
^d Also at TRIUMF, Vancouver, BC, Canada.
^e Also at Department of Physics & Astronomy, University of Louisville, Louisville, KY, United States.
^f Also at Physics Department, An-Najah National University, Nablus, Palestine.
^g Also at Department of Physics, California State University, Fresno, CA, United States.
^h Also at Department of Physics, University of Fribourg, Fribourg, Switzerland.
ⁱ Also at II Physikalisches Institut, Georg-August-Universität, Göttingen, Germany.
^j Also at Departament de Física de la Universitat Autònoma de Barcelona, Barcelona, Spain.
^k Also at Departamento de Física e Astronomia, Faculdade de Ciências, Universidade do Porto, Portugal.
^l Also at Tomsk State University, Tomsk, and Moscow Institute of Physics and Technology State University, Dolgoprudny, Russia.
^m Also at The Collaborative Innovation Center of Quantum Matter (CICQM), Beijing, China.
ⁿ Also at Università di Napoli Parthenope, Napoli, Italy.
^o Also at Institute of Particle Physics (IPP), Canada.
^p Also at Horia Hulubei National Institute of Physics and Nuclear Engineering, Bucharest, Romania.
^q Also at Department of Physics, St. Petersburg State Polytechnical University, St. Petersburg, Russia.
^r Also at Borough of Manhattan Community College, City University of New York, New York City, United States.
^s Also at Department of Financial and Management Engineering, University of the Aegean, Chios, Greece.
^t Also at Centre for High Performance Computing, CSIR Campus, Rosebank, Cape Town, South Africa.
^u Also at Louisiana Tech University, Ruston, LA, United States.
^v Also at Institutio Catalana de Recerca i Estudis Avançats, ICREA, Barcelona, Spain.
^w Also at Department of Physics, The University of Michigan, Ann Arbor, MI, United States.
^x Also at Graduate School of Science, Osaka University, Osaka, Japan.
^y Also at Fakultät für Mathematik und Physik, Albert-Ludwigs-Universität, Freiburg, Germany.
^z Also at Institute for Mathematics, Astrophysics and Particle Physics, Radboud University Nijmegen/Nikhef, Nijmegen, Netherlands.
^{aa} Also at Department of Physics, The University of Texas at Austin, Austin, TX, United States.
^{ab} Also at Institute of Theoretical Physics, Ilia State University, Tbilisi, Georgia.
^{ac} Also at CERN, Geneva, Switzerland.
^{ad} Also at Georgian Technical University (GTU), Tbilisi, Georgia.
^{ae} Also at O Chadai Academic Production, Ochanomizu University, Tokyo, Japan.
^{af} Also at Manhattan College, New York, NY, United States.
^{ag} Also at The City College of New York, New York, NY, United States.
^{ah} Also at Departamento de Física Teórica y del Cosmos, Universidad de Granada, Granada, Spain.
^{ai} Also at Department of Physics, California State University, Sacramento, CA, United States.
^{aj} Also at Moscow Institute of Physics and Technology State University, Dolgoprudny, Russia.
^{ak} Also at Departement de Physique Nucleaire et Corpusculaire, Université de Genève, Geneva, Switzerland.
^{al} Also at Institut de Física d'Altes Energies (IFAE), The Barcelona Institute of Science and Technology, Barcelona, Spain.
^{am} Also at School of Physics, Sun Yat-sen University, Guangzhou, China.
^{an} Also at Institute for Nuclear Research and Nuclear Energy (INRNE) of the Bulgarian Academy of Sciences, Sofia, Bulgaria.
^{ao} Also at Faculty of Physics, M.V. Lomonosov Moscow State University, Moscow, Russia.
^{ap} Also at National Research Nuclear University MEPhI, Moscow, Russia.
^{aq} Also at Department of Physics, Stanford University, Stanford, CA, United States.
^{ar} Also at Institute for Particle and Nuclear Physics, Wigner Research Centre for Physics, Budapest, Hungary.
^{as} Also at Giresun University, Faculty of Engineering, Turkey.
^{at} Also at CPPM, Aix-Marseille Université and CNRS/IN2P3, Marseille, France.
^{au} Also at Department of Physics, Nanjing University, Jiangsu, China.
^{av} Also at Institute of Physics, Academia Sinica, Taipei, Taiwan.
^{aw} Also at University of Malaya, Department of Physics, Kuala Lumpur, Malaysia.
^{ax} Also at LAL, Univ. Paris-Sud, CNRS/IN2P3, Université Paris-Saclay, Orsay, France.
^{*} Deceased.